Spontaneous Breaking of Translational Invariance and Spatial Condensation in Stationary States on a Ring
I. The Neutral System

Peter F. Arndt[⋆§], Thomas Heinzel[⋆] and Vladimir Rittenberg[⋆†]

[⋆] Physikalisches Institut
Nußallee 12, 53115 Bonn, Germany

[†] SISSA
Via Beirut 2–4, 34014 Trieste, Italy

[§]Institut für Theoretische Physik
Universität zu Köln, Zülpicher Str. 77, 50937 Köln, Germany

We consider a model in which positive and negative particles with equal densities diffuse in an asymmetric, CP invariant way on a ring. The positive particles hop clockwise, the negative counter-clockwise and oppositely-charged adjacent particles may swap positions. The model depends on two parameters.

Analytic calculations using quadratic algebras, inhomogeneous solutions of the mean-field equations and Monte-Carlo simulations suggest that the model has three phases. A pure phase in which one has three pinned blocks of only positive, negative particles and vacancies and in which translational invariance is broken. A mixed phase in which the current has a linear dependence on one parameter but is independent of the other one and of the density of the charged particles. In this phase one has a bump and a fluid. The bump (condensate) contains positive and negative particles only, the fluid contains charged particles and vacancies uniformly distributed. The mixed phase is separated from the disordered phase by a second-order phase-transition which has many properties of the Bose-Einstein phase-transition observed in equilibrium. Various critical exponents are found.

Keywords: non-equilibrium statistical mechanics, phase transitions, spontaneous symmetry breaking, condensation, quadratic algebras

1. Introduction

While the conceptual framework for the understanding of spontaneous symmetry breaking (SSB) occurring in systems at thermal equilibrium is well established, it is much poorer for systems far from equilibrium. It was realized recently though, that exclusion models with hard core interaction, are simple enough to allow analytic methods, either approximative or exact, for the description of their stationary states, yet exhibit a rich variety of behaviors even in one dimension. For example SSB of CP symmetry in a first-order phase transition was observed in open systems with two [1, 2, 3] or three species [4, 5].

The aim of the present work is to analyze the structure of the stationary states of a one-dimensional three-species exclusion model on a ring with continuous symmetries and, in particular, to address the question of the existence of SSB. In this model, introduced in [6], positive and negative particles diffuse in an asymmetric, CP invariant way. The positive particles hop clockwise, the negative particles counter-clockwise and oppositely charged adjacent particles may exchange positions. The model thus defined is translationally invariant and the numbers of positive and negative particles are conserved. The study presented in [6] suggests the existence of three phases in the stationary state. In particular, as we shall see, for two of these phases charge segregation (segregation of species) occurs in the system. Here we confirm these predictions, we provide a more complete analysis of these phases and try to unravel the mechanisms by which phase transitions occur in such a simple system. A summary of the features of the phases and of the phenomenology of the model is given below. We first come back to its definition.

We consider a ring of L sites, labeled by $k = 1, \ldots, L$. Each site is occupied by one of the three types of particles, 0, 1 or 2. The particle of type 0 is hereafter referred to as a vacancy. The dynamics of the model is defined as follows. At each time step a bond is chosen randomly, and the particles α and β located at the two ends of the bond exchange positions with the rate $g_{\alpha,\beta}$, where the indices $\alpha, \beta = 0, 1, 2$. Therefore, the dynamics conserves the number of particles N_α of each species. Up to this point, this defines a class of models depending on five parameters, since rates are defined up to a rescaling of time. Here we restrict the model taking the following rates

$$
\begin{aligned}
(1)(0) &\to (0)(1) &&\text{with rate } g_{1,0} = \lambda \\
(0)(2) &\to (2)(0) &&\text{with rate } g_{0,2} = \lambda \\
(2)(1) &\to (1)(2) &&\text{with rate } g_{2,1} = 1 \\
(1)(2) &\to (2)(1) &&\text{with rate } g_{1,2} = q
\end{aligned}
\tag{1.1}
$$

i.e. the remaining rates $g_{0,1}$ and $g_{2,0}$ are zero. The model depends on two parameters λ and q (for convenience, we introduce also the parameter $r = 1/q$). In order to facilitate the intuitive description of the model, we will also denote the particles of type 1 and 2 by $(+)$ and $(-)$ respectively and rewrite (1.1) as

$$g_{+,0} = g_{0,-} = \lambda, \qquad g_{-,+} = 1, \qquad g_{+,-} = q \tag{1.2}$$

In what follows we will consider only the case of equal densities of charged particles that we are going to denote by ρ. With the choice of rates (1.2), we expect therefore the stationary state to be CP invariant and the currents of positive and negative particles to be equal. The case of unequal densities is subject of a separate paper [7].

For the sake of clarity, we present here a summary of the main phenomenological features of this model, using a simple intuitive presentation. Our knowledge is based on the study of the model by exact algebraic methods, mean-field analysis and Monte-Carlo simulations, described in the later sections. For a given density ρ, the phase diagram of the model consists of three sectors in the $q - \lambda$ plane.

The *pure phase*. $(0 < q < 1$, any λ and $\rho)$. If one takes a system of size L and start from an arbitrary configuration, in the long time regime, the system organizes itself into three blocks

$$(\,0\,)\cdots(\,0\,)(+)\cdots(+)(-)\cdots(-) \tag{1.3}$$

building what we are going to call a bump which covers the whole ring. This may be simply understood looking at the rates (1.2). Since $q < 1$, in the average, particles of type $(-)$ will be preferentially located to the right of particles of type $(+)$. Themselves will be found to the right of particles of type $(\,0\,)$, while the latter will be found on the ring to the right of particles of type $(-)$. The average waiting time between hops of the bumps from one position on the ring to another one increase exponentially with L. Let us give an intuitive explanation of this point. Prepare the system as in (1.3). According to (1.2) the single bond that is allowed to evolve is the one located at the interface between the positive and negative blocks. Consider the positive particle at the interface. It will begin diffusing through the negative block to its right, but with a bias to the left since $q < 1$, resulting in a restoring force on the particle. As a consequence, the probability for this particle to transverse the negative block is exponentially decreasing with the size of the system. In the thermodynamic limit, any configuration (1.3) on the ring is an absorbing state of the dynamics, i.e. the system does not evolve. Otherwise stated, the configuration space is decomposed into a continuous infinity of "ergodic" components, i.e. ergodicity is infinitely broken. As a consequence, in the thermodynamic limit, translational invariance is broken, the current is zero and the segregation of charges maximal, corresponding to a complete charge segregation (hence the name pure phase). Let us observe that, in general, if one denotes by $c_{\alpha,\beta}(R, L)$ any connected two-point

function for a system of size L and if instead of the distance R one takes the dimensionless variable $y = R/L$, charge segregation implies that the limits

$$\lim_{L \to \infty} c_{\alpha,\beta}(R, L) = \lim_{L \to \infty} c_{\alpha,\beta}(y, L) = c_{\alpha,\beta}(y) \tag{1.4}$$

exist (similar limits exist also for any n-point functions). Charge segregation was seen in two [1, 3, 2, 8] and three-species [5] open systems when first-order phase transitions take place. In the present case the functions $c_{\alpha,\beta}(y)$ have a simple expression which can be computed using (1.3). The pure phase was seen also in Ref.[9] for $\rho = 1/3$ in a different model where the rates are

$$g_{1,0} = g_{0,2} = g_{2,1} = 1, \qquad g_{0,1} = g_{2,0} = g_{1,2} \tag{1.5}$$

The finite-size behavior of the present model and that of Ref.[9] are different.

The *mixed phase*. For fixed λ and ρ, this phase appears as soon as $1 < q$ and survives until q reaches a critical value

$$q_c = 1 + \frac{4\lambda\rho}{1 + 2\rho} \tag{1.6}$$

Again segregation of species is observed, though differently from what was observed previously for $q < 1$. In order clarify the physics let us take q larger but close to 1. The two blocks of $(+)$ and $(-)$ particles, which were distinct in the pure phase, merge in one region, hereafter called condensate. The rest of the system, hereafter called fluid, is mainly occupied by vacancies and traversed by a few $(+)$ and $(-)$ particles distributed in an uniform way. This may be understood as follows. Prepare the system in the configuration (1.3). The only particles that can move are located at the $(+)(-)$ interface. The difference is that now the bias, proportional to $q - 1$, is positive, i.e. oriented to the right. Therefore the $(+)$ particle has a finite probability to traverse the negative block on its right. As soon as a $(+)$ particle leaves the condensate at its right end, it reappears almost instantly at its left end. In other words the positive component of the condensate melts on the right but is restored on the left. At the left hand side of the condensate the density profile of positive particles is close to one while small on the right hand side. The same reasoning holds for the negative particles, we just have to exchange the word right with left. Hence it is clear that the condensate as a whole moves diffusively on the ring and therefore translational invariance is not broken. Finite-size effects are much more important in the mixed phase than in the pure phase. In the thermodynamical limit, in the condensate, the densities $(+)$ and $(-)$ particles are both equal to 1/2, hence the condensate can be seen as a two species system with open boundaries in the "maximal current phase". In the "maximal current phase", the current has the expression

$$J = \frac{q - 1}{4} \tag{1.7}$$

which is precisely the value of the current observed in the whole mixed phase. The condensate is glued to the fluid where all three species are present and distributed in a uniform way. If we let now vary q from 1 to q_c, keeping λ and ρ constant, the condensate shrinks and the fluid takes over the whole ring at q_c. In the whole mixed phase one has charge segregation since the limit (1.4) exists. This brings us to two types of charge segregation on the ring. One in which translational invariance is broken (type B), like in the pure phase and another one in which translational invariance is unbroken (type UB), like in the mixed phase.

The *disordered phase* occurs when $q > q_c$, the current has a non trivial dependence on the density. The density profiles are uniform and there is no charge segregation.

A lot of work was done previously on the three species diffusion problem in other models, especially in two dimensions (see for example Ref.[10] and references included). The present model is interesting for two reasons. First, this model has the phase structure we just mentioned, secondly, the stationary states of this model can be studied using the powerful method of quadratic algebras. This not only allows to obtain precise results but also allows the introduction of computational methods, like the grand canonical ensemble which can not be defined otherwise. This forces us to present our results starting with some mathematics.

In Sec.2 we first review some results obtained in Ref.[11] where it was shown that for the rates (1.1), the probability distribution for the stationary state can be obtained by taking traces of monomials of generators of a specific quadratic algebra. We give the representations of this algebra. They are in general infinite-dimensional unless λ is related to q. We next show how to do calculations in the canonical ensemble and explain why this approach can be applied only to small lattices. A grand canonical ensemble is defined using the algebra. It is stressed that this definition is not unique but very useful. We also show a novel application of the algebra which gives the large q (small r) expansions of different physical quantities. A connection between the representations of the quadratic algebra and the quantum algebra $U_q so(2,1)$ is given in Appendix A.

In Sec.3 we give the values of the currents in the three phases using mainly Monte-Carlo simulations for the canonical ensemble and algebraic methods for the grand canonical ensemble. We also discuss the problem of fine-size corrections.

The two-point correlation functions for the pure and mixed phase are presented in Secs.4 and 5.

Mean-field calculations are presented in Appendix B and in Sec.6 first on the lattice and then in the continuum. The latter are interesting on their own because we obtain stationary solutions of two coupled non-linear differential equations in which the size L of the system is a parameter. The mean-field results are compared with various results obtained through other methods.

In Sec.7 we define an complex order parameter that we denote by M and compute the Ginzburg-Landau potential defined in Ref.[5] (there it was called free energy functional) as a function of $|M|$. A minimum at a non-zero value of $|M|$ of the Ginzburg-Landau potential would imply charge segregation. This is indeed seen for both the pure and mixed phase but not, as expected, in the disordered phase. If we look however for a system of size L at the average time T to move from a domain in the complex M-plane to another, we observe that T depends exponentially on L in the pure phase and algebraically in the mixed phase. This implies that translational invariance is spontaneously broken in the pure phase but not in the mixed phase.

At q_c a second-order phase transition takes place. The values of several critical exponents are given in Sec.8. It is also shown that, like in the case of Bose-Einstein condensation (reviewed in Appendix C), at q_c the fugacities do not determine the densities.

A detailed study of the phenomenon of spatial condensation is given in Sec.9. We show the L dependence of the compressibility and the Ginzburg-Landau potential as a function of the local density of vacancies. We also show that, amazingly, one can define a quantity which behaves like the pressure in equilibrium systems. Based on what is done in the case of Bose-Einstein condensation, we give a way to eliminate the condensate and keep only the fluid in the mixed phase.

Our conclusions are given in Sec.10.

2.   The quadratic algebra and its applications.

In this section we show how to use the algebraic methods, pioneered by Affleck et al [12] for equilibrium problems and by Hakim and Nadal [13] and Derrida et al [3] for non-equilibrium problems, to describe the stationary probability distribution obtained from the master equation given by the rates (1.1).

In Ref.[11] it was shown for which rates $g_{\alpha\beta}$ the unnormalized stationary probability distribution $P_s(\beta_1, \beta_2, \ldots, \beta_L)$ of a three-state problem with L sites on a ring is given by the expression:

$$P_s(\beta_1, \beta_2, \ldots, \beta_L) = \mathrm{Tr}(D_{\beta_1} D_{\beta_2} \cdots D_{\beta_L}) \qquad (\beta_k = 0, 1, 2) \qquad (2.1)$$

where the D_α's satisfy the quadratic algebra:

$$g_{\alpha\beta} D_\alpha D_\beta - g_{\beta\alpha} D_\beta D_\alpha = x_\beta D_\alpha - x_\alpha D_\beta \qquad (2.2)$$

The cases for which the algebra (2.2) exists and has representations with a finite trace can be classified depending on how many of the parameters x_α are zero. In particular, it was shown that for the rates considered in this paper, the probability distribution can be obtained by the ansatz (2.1)–(2.2) with $x_0 = 0$ (See Ref. [11], Eqs.(3.30)–(3.47)). In

this case, the quadratic algebra takes the simple form:

$$G_1 G_2 = r(G_2 G_1 + \lambda(G_1 + G_2))$$
$$G_1 G_0 = G_0$$
$$G_0 G_2 = G_0 \tag{2.3}$$

where

$$D_0 = d_0 G_0 , \qquad D_1 = d_1 G_1 , \qquad D_2 = d_2 G_2 \tag{2.4}$$

d_0, d_1 and d_2 are free parameters (the freedom in choosing x_1 and x_2 was taken into account). The existence of the free parameters is a consequence of the conservation of the numbers of particles N_1 and N_2.

We will first review the representations of the algebra (2.3) obtained in Ref. [11] and then explain how they can be used to compute various physical quantities. We will also show how to use the algebra (2.3) to obtain a large q (small r) expansion and derive expressions for the current. It turns out that in some cases, G_1 and G_2 can be expressed in terms of generators of the quantum algebra $U_q(so(2,1))$. In Appendix A we show how this information can be used.

2.1. Representations of the quadratic algebra.

As discussed already in Ref.[11], we are interested for a given value of λ and r in representations of the smallest dimension.

A one-dimensional representation (this is equivalent to a product measure probability distribution) is obtained for any λ and r:

$$G_0 = 0 , \qquad G_1 = \gamma_1 , \qquad G_2 = \gamma_2 \tag{2.5}$$

with

$$\gamma_2 = \frac{r\lambda\gamma_1}{\gamma_1(1-r) - \lambda r} . \tag{2.6}$$

Here γ_1 and γ_2 are c-numbers. Since $G_0 = 0$, one has no vacancies and one has only an asymmetric exclusion process.

If G_0 is non-vanishing it is convenient to denote

$$G_1 = \mathcal{A} + \mathcal{U} , \qquad G_2 = \mathcal{A} + \mathcal{V} \tag{2.7}$$

and a representation is given by:

$$G_0 = \begin{pmatrix} 1 & 0 & 0 & 0 & \cdots \\ 0 & 0 & 0 & 0 & \\ 0 & 0 & 0 & 0 & \\ 0 & 0 & 0 & 0 & \\ \vdots & & & & \ddots \end{pmatrix} , \qquad \mathcal{A} = \begin{pmatrix} a_1 & 0 & 0 & 0 & \cdots \\ 0 & a_2 & 0 & 0 & \\ 0 & 0 & a_3 & 0 & \\ 0 & 0 & 0 & a_4 & \\ \vdots & & & & \ddots \end{pmatrix}$$

$$
\mathcal{U} = \begin{pmatrix} 0 & t_1 & 0 & 0 & \cdots \\ 0 & 0 & t_2 & 0 & \\ 0 & 0 & 0 & t_3 & \\ 0 & 0 & 0 & 0 & \ddots \\ \vdots & & & & \ddots \end{pmatrix} , \qquad
\mathcal{V} = \begin{pmatrix} 0 & 0 & 0 & 0 & \cdots \\ s_1 & 0 & 0 & 0 & \\ 0 & s_2 & 0 & 0 & \\ 0 & 0 & s_3 & 0 & \\ \vdots & & & \ddots & \ddots \end{pmatrix} \tag{2.8}
$$

with

$$
a_k = r\left[(\lambda+1)\{k-1\}_r - \{k-2\}_r\right]
$$
$$
s_k\, t_k = \{k\}_r \left[(2\lambda+1)r - 1 + (r(\lambda+1)-1)^2 \{k-1\}_r\right] . \tag{2.9}
$$

We have used the notation

$$
\{k\}_r = \frac{r^k - 1}{r - 1} . \tag{2.10}
$$

The representations given by Eq.(2.8) are not necessarily infinite dimensional. One can obtain an n-dimensional representation by finding the solutions of the equation:

$$
s_n\, t_n = 0 . \tag{2.11}
$$

Using Eqs.(2.9) and (2.11) we obtain:

$$
\lambda = \frac{1 - r}{r(1 + r^{\frac{1-n}{2}})} \tag{2.12}
$$

The n-dimensional representation has the following matrix elements $(k = 1, 2, \ldots, n)$

$$
a_k = \frac{1 + r^{k - \frac{1+n}{2}}}{1 + r^{\frac{1-n}{2}}}
$$
$$
s_k\, t_k = \frac{(1 - r^k)(1 - r^{k-n})}{\left(1 + r^{\frac{1-n}{2}}\right)^2} . \tag{2.13}
$$

Let us observe that from Eq.(2.12) we get a one-dimensional representation, $n = 1$, with $G_0 = G_1 = G_2 = 1$ if

$$
q = 2\lambda + 1 . \tag{2.14}
$$

Notice that in this is case G_0 is non-zero! A two-dimensional representation, $n = 2$, is obtained if

$$
q = (1 + \lambda)^2 \tag{2.15}
$$

and one can choose the basis such that one has

$$
\mathcal{A} = \begin{pmatrix} 1 & 0 \\ 0 & \sqrt{r} \end{pmatrix} , \quad
\mathcal{U} = \begin{pmatrix} 0 & 1 - \sqrt{r} \\ 0 & 0 \end{pmatrix} , \quad
\mathcal{V} = \begin{pmatrix} 0 & 0 \\ \sqrt{r} - 1 & 0 \end{pmatrix} . \tag{2.16}
$$

A second two-dimensional representation is also obtained for any λ if $r = 0$. In this case one has to take $r = 0$ in the expressions for $\mathcal{A}$, $\mathcal{U}$ and $\mathcal{V}$ in Eq.(2.16). This observation will be useful in Sec.2.4.

To sum up, we have a one-dimensional representation with $G_0 = 0$ for any λ and q and a second one-dimensional representation with $G_0 \neq 0$ when q and λ are related by Eq.(2.14). We also have two two-dimensional representations. One corresponds to Eq.(2.15), the second one is obtained for $r = 0$. For $n \geq 3$, one has only one n-dimensional representation when Eq.(2.12) is satisfied. For generic q and λ and $G_0 \neq 0$ the representations are infinite-dimensional.

Due to the special structure of the representations with trace of the algebra (2.3), the expression (2.1) has to be used with care. If one looks at configurations with no vacancies, one has to use the one-dimensional representation (2.5). For any configuration which contains at least one vacancy one has to use the representation given by Eqs.(2.7)-(2.8) which, as discussed, can be finite or infinite-dimensional depending on the values of q and λ.

2.2. The canonical ensemble.

In this case the numbers of particles N_1 and N_2 are given. The normalized probability distribution can be obtained from Eqs.(2.1) and (2.4):

$$P^{\mathrm{c}}_{N_1,N_2}(\beta_1, \beta_2, \ldots, \beta_L) = \frac{1}{Z_L^{N_1,N_2}} F^{\mathrm{c}}_{N_1,N_2}(\beta_1, \beta_2, \ldots, \beta_L) \,, \tag{2.17}$$

where $Z_L^{N_1,N_2}$ is a normalization factor and

$$F^{\mathrm{c}}_{N_1,N_2}(\beta_1, \beta_2, \ldots, \beta_L) = \mathrm{Tr}(G_{\beta_1} G_{\beta_2} \cdots G_{\beta_L})$$
$$\times \delta(\sum_{k=1}^{L} \delta(\beta_k - 1) - N_1)\, \delta(\sum_{k=1}^{L} \delta(\beta_k - 2) - N_2) \tag{2.18}$$

where $\delta(x)$ is the Kronecker function.

The currents are going to play an important role in this paper. They are defined as follows: The current for the particles of type 1, taken for convenience on the link between the sites $L - 1$ and L, is:

$$j_1 = \lambda\, \delta(\beta_{L-1} - 1)\, \delta(\beta_L) + q\, \delta(\beta_{L-1} - 1)\, \delta(\beta_L - 2) - \delta(\beta_{L-1} - 2)\, \delta(\beta_L - 1) \tag{2.19}$$

The current for the type 2 particles has a similar expression. Using the Eqs.(2.17)-(2.19) and (2.3), the expression for the average current is:

$$J_1 = \frac{\lambda}{Z_L^{N_1,N_2}} \sum_{\beta_1,\ldots,\beta_{L-2}} [\mathrm{Tr}(G_{\beta_1} G_{\beta_2} \cdots G_{\beta_{L-2}} G_0)$$
$$\times \delta(\sum_{k=1}^{L-2} \delta(\beta_k - 1) - N_1 + 1)\, \delta(\sum_{k=1}^{L-2} \delta(\beta_k - 2) - N_2)$$

$$+\text{Tr}(G_{\beta_1} G_{\beta_2} \cdots G_{\beta_{L-2}} (G_1 + G_2))$$

$$\times\delta(\sum_{k=1}^{L-2} \delta(\beta_k - 1) - N_1 + 1)\,\delta(\sum_{k=1}^{L-2} \delta(\beta_k - 2) - N_2 + 1)] \qquad (2.20)$$

It is useful to employ the Fourier transform of the Kronecker delta function

$$\delta(\alpha) = \frac{1}{L} \sum_{k=0}^{L-1} \exp(\frac{2\pi\mathrm{i}}{L} k\alpha) \qquad\qquad (\alpha = 0, \dots, L-1) \qquad (2.21)$$

and to define

$$B_{r,s}^{(L)} = G_0 + \exp(\frac{2\pi\mathrm{i}}{L} r)G_1 + \exp(\frac{2\pi\mathrm{i}}{L} s)G_2 \ . \qquad (2.22)$$

In this way one can get a compact expression for the current of type 1 particles. The expressions for the type 2 particles and for the normalisation factor $Z_L^{N_1,N_2}$ can be obtained in a similar way. One obtains:

$$Z_L^{N_1,N_2} = \frac{1}{L^2} \sum_{r,s=0}^{L-1} \exp\left(-2\pi\mathrm{i}\left(r\frac{N_1}{L} + s\frac{N_2}{L}\right)\right) \text{Tr}\left((B_{r,s}^{(L)})^L\right) \qquad (2.23)$$

$$J_1 = \frac{\lambda}{Z_L^{N_1,N_2}} \sum_{r,s=0}^{L-3} \exp\left(-2\pi\mathrm{i}\left(r\frac{N_1-1}{L-2} + s\frac{N_2}{L-2}\right)\right) \text{Tr}\left((B_{r,s}^{(L-2)})^{L-2} B_{s,s}^{(L-2)}\right) \qquad (2.24)$$

$$J_2 = \frac{\lambda}{Z_L^{N_1,N_2}} \sum_{r,s=0}^{L-3} \exp\left(-2\pi\mathrm{i}\left(r\frac{N_1}{L-2} + s\frac{N_2-1}{L-2}\right)\right) \text{Tr}\left((B_{r,s}^{(L-2)})^{L-2} B_{r,r}^{(L-2)}\right) \qquad (2.25)$$

Analogous expressions can be written for the correlation functions.

In a concrete calculation (q and λ are given) we take G_0, G_1 and G_2 from Eqs.(2.8) and (2.9). This gives the matrices $B_{r,s}^{(L)}$ of Eq.(2.22) and we are left with the calculation of the traces appearing in Eqs.(2.23)-(2.25) and the double summations over r and s. We have been unable to do any analytical calculation in this way in the general case (for finite dimensional representations this is probably possible). This takes us to numerical calculations. If we take $N_1 + N_2 \neq L$, the trace operation in Eq.(2.20) is well defined and any divergence in Eqs. (2.23)-(2.25) has to cancel, this does not make however numerical evaluations easy. To circumvent the problem of computing traces of infinite dimensional matrices we will assume that we have at least one vacancy and take in Eq.(2.23) $\text{Tr}(G_0(B_{r,s}^{(L-1)})^{L-1}) \equiv \{(B_{r,s}^{(L-1)})^{L-1}\}_{1,1}$ instead of $\text{Tr}((B_{r,s}^{(L)})^L)$ and $L-1$ instead of L. The expressions for the currents have to changed in the same sense. Due to the fact that G_0 is a projector (see Eq. (2.8)) this procedure has also the advantage that for a problem with L sites, only the matrix elements with $k < L$ (see Eq.(2.8)) appear in the evaluation of the traces. In this way we have been able to compute the current up to $L = 30$ with high precision. This allows in principle, using extrapolants [14], to obtain the current in the thermodynamical limit. As will be shown in Sec.3 the current might converge very slowly towards its thermodynamical limit and therefore in

these cases this method is useless. As a matter of fact, throughout this paper, we have used Monte-Carlo simulations for the canonical ensemble. The precision is much worse than using the analytical method but one can reach much larger values of L.

2.3. The grand canonical ensemble.

As opposed to equilibrium states, the definition of a grand canonical ensemble for stationary states is not unique. In principle, for the master equation one can give, at $t = 0$, an initial probability distribution in which the number of particles N_1 and N_2 are not fixed but the "chemical potentials" μ_1 and μ_2 are. Such an initial probability distribution has the expression:

$$P^{gc}_{\mu_1,\mu_2}(\beta_1,\ldots,\beta_L,t=0) = \sum_{N_1,N_2} Q(\beta_1,\ldots,\beta_L; N_1, N_2)e^{\mu_1 N_1 + \mu_2 N_2} \qquad (2.26)$$

where Q is an arbitrary function. This initial condition determines a certain stationary probability that can be considered as a grand canonical ensemble. The N_1 and N_2 dependence of the functions Q remains however arbitrary even if we make sure that the average densities $\rho_1 = <N_1> /L$ and $\rho_2 = <N_2> /L$ are properly obtained. We will adopt a different approach looking directly at the canonical stationary distribution given by Eq.(2.17) and consider the grand canonical ensemble defined by the expression:

$$P^{gc}_{\mu_1,\mu_2}(\beta_1,\ldots,\beta_L) = \frac{1}{Z_L^{\mu_1,\mu_2}} \sum_{N_1,N_2} \frac{F^c_{N_1,N_2}(\beta_1,\beta_2,\ldots,\beta_L)}{f^L_{N_1,N_2}} e^{\mu_1 N_1 + \mu_2 N_2} \qquad (2.27)$$

where we have used Eq.(2.18). In Eq.(2.27) the factors $f^L_{N1,N2}$ are arbitrary. We will take from now on:

$$f^L_{N_1,N_2} = 1 \qquad (2.28)$$

A similar definition was used in [15]. This gives:

$$P^{gc}_{\mu_1,\mu_2}(\beta_1,\ldots,\beta_L) = \frac{1}{Z_L^{\mu_1,\mu_2}} \mathrm{Tr}(E_{\beta_1} \cdots E_{\beta_L}) \qquad (2.29)$$

where

$$E_0 = G_0, \qquad E_1 = z_1 G_1, \qquad E_2 = z_2 G_2 \qquad (2.30)$$

and

$$z_1 = e^{\mu_1}, \qquad z_2 = e^{\mu_2} \qquad (2.31)$$

are the fugacities. As opposed to the canonical ensemble, the grand canonical partition function has a simple expression:

$$Z_L^{\mu_1,\mu_2} = \mathrm{Tr}\left(C^L\right) \qquad (2.32)$$

where

$$C = E_0 + E_1 + E_2 .$$
(2.33)

That this choice for the definition of the grand canonical ensemble is not unique can be seen in a different way. Instead of using the D's of Eq.(2.4) with $d_0 = d_1 = d_2 = 1$ (for the canonical ensemble this choice is not important), we could have taken $d_0 = 1$ (one of the d_i can be chosen at will) but keep d_1 and d_2 as free parameters. In this case, Eq.(2.30) is replaced by

$$E_0 = G_0, \qquad E_1 = d_1 z_1 G_1, \qquad E_2 = d_2 z_2 G_2$$
(2.34)

and all the results for finite-size systems will be affected, but hopefully not the results for the thermodynamical limit. We want to stress this point because the interpretation of finite-size corrections for the grand canonical ensemble has still to be understood. We have arbitrarily taken the choice given by Eq.(2.28). Our choice promotes the algebra (2.3) to a special role, since the isomorphic algebras obtained using various values of the d_i in Eq.(2.4) give different definitions of the grand canonical ensemble. We have no good reason to prefer one algebra to the other except the fact that the representation of the algebra (2.3) can be connected "naturally" to known representations of quantum algebras (see Appendix A).

The expression (2.29) reminds us of an analogous expression in equilibrium statistical physics and along this line of thought, one could perhaps find a better justification for a proper definition of the grand canonical ensemble. That this idea is not too far fetched will be seen in Sec.9.

We now proceed with the description of the grand canonical ensemble. As usual the fugacities are fixed by the densities:

$$\rho_i = \frac{< N_i >}{L} = \frac{z_i}{L} \frac{\partial \log Z_L^{\mu_1,\mu_2}}{\partial z_i}$$
(2.35)

The fluctuations of the densities are:

$$< (\Delta N_i)^2 > = \frac{\partial^2 \log Z_L^{\mu_1,\mu_2}}{\partial \log z_i{}^2}$$
(2.36)

Using Eqs.(2.29) and (2.33), one gets the two-point functions:

$$c_{\alpha,\beta}(R) = \frac{1}{Z_L^{\mu_1,\mu_2}} \text{Tr}(G_\alpha C^{R-1} G_\beta C^{L-R-1})$$
(2.37)

Notice that if the matrix C has the two largest eigenvalues $\lambda_1 > \lambda_2$ and if these eigenvalues are not degenerate, at large distances R the two point function has the expression:

$$c_{\alpha,\beta}(R) \propto \exp(-MR)$$
(2.38)

where the inverse correlation length M is:

$$M = \log \frac{\lambda_1}{\lambda_2} \qquad (2.39)$$

This implies that for finite-dimensional representations (see Eq.(2.13)) one expects finite correlation lengths. This conjecture can be proven rigorously but it is a lengthy exercise that we have not done. The expression of the currents can be derived using Eqs.(2.19) and (2.3). We get

$$J_1 = \frac{\lambda z_1}{Z_L^{\mu_1,\mu_2}} \mathrm{Tr}\left((G_0 + z_2(G_1 + G_2))C^{L-2} \right) \ . \qquad (2.40)$$

The expression for J_2 is obtained by permuting 1 with 2 in Eq.(2.40). If we consider the case in which the densities of the particles 1 and 2 are the same, the expression of the currents takes a very simple form:

$$J_1 = J_2 = \lambda z \frac{Z_{L-1}^{\mu,\mu}}{Z_L^{\mu,\mu}} \qquad (2.41)$$

where

$$z = e^{\mu} \ . \qquad (2.42)$$

This makes the calculation of the current much simpler in the grand canonical ensemble.

In the expressions written above (see (2.32), (2.37) and (2.40)), we have made the assumption that the trace operation exists. This is clearly the case if one has finite-dimensional representations. The case of infinite-dimensional representations has to be considered with care. In the grand canonical ensemble, for a given number of sites L one sums over the values N_1 and N_2. In this sum there is also the term with $N_1 + N_2 = L$ where no G_0 matrix appears (2.18) and one has only products of G_1 and G_2 matrices given by Eq.(2.8) which have no trace. One has to use for this case the representation (2.5) which makes the calculation cumbersome. A simpler way is to define the grand canonical ensemble such that one has at least one vacancy. That is what we have done. In this case, one has to sum over all possibilities for the relative position of the G_0 matrix and the operator whose expectation value one wants to compute (see Eqs.(2.32),(2.37) and (2.40)). For each term, taking into account the form of the matrix G_0 (see Eq.(2.8)), one replaces the trace operation by taking an appropriate $(1,1)$ matrix element. Like in the canonical ensemble, we have not been able to do analytical calculations and had to use the computer but in the grand canonical ensemble we were able to reach $L = 300$, as opposed to $L = 30$ for the canonical ensemble.

2.4. The large q expansion in the grand canonical ensemble.

A useful application of the algebra (2.3) is that one can do a large q (small r) expansion in an algebraic way. We will show how to obtain the physical quantities up to order r.

We first note that, if we keep terms up to order r in the matrix elements (2.9) which give G_1 and G_2, the only non-vanishing elements are

$$a_1 = 1 , \qquad a_2 = (1 + \lambda)r , \qquad a_k = \lambda r \quad (k \geq 3)$$
$$s_1 t_1 = (2\lambda + 1)r - 1 , \qquad s_2 t_2 = -r \tag{2.43}$$

Since one is interested in the smallest representation, it is enough to take a 3×3 dimensional one. One can check that taking this representation one obtains:

$$G_1 G_2 - r \left(G_2 G_1 + \lambda(G_1 + G_2) \right) = r^{\frac{3}{2}} \begin{pmatrix} 0 & 0 & 0 \\ 0 & 0 & -(1+\lambda) \\ 0 & (1+\lambda) & 0 \end{pmatrix} \tag{2.44}$$

which shows the consistency of the approach since the right-hand-side of Eq. (2.44) is of order $r^{3/2}$. We have chosen a representation in which $\mathcal{U} = -\mathcal{V}^T$ (see Eq.(2.8)). Notice that if we neglect the terms of order r, we obtain the two dimensional representation (2.16) in which we take $r = 0$.

We will consider only the grand canonical ensemble and assume that the densities of particles 1 and 2 are the same:

$$\rho = \rho_1 = \rho_2 \tag{2.45}$$

The matrix C given by Eq.(2.32) becomes

$$C = \begin{pmatrix} 1 + z_1 + z_2 & z_1(1 - \frac{2\lambda+1}{2}r) & 0 \\ -z_2(1 - \frac{2\lambda+1}{2}r) & (1+\lambda)(z_1 + z_2)r & z_1 r^{\frac{1}{2}} \\ 0 & -z_1 r^{\frac{1}{2}} & \lambda(z_1 + z_2)r \end{pmatrix} . \tag{2.46}$$

We are interested to obtain the coefficients of the r-expansion defined by the expressions:

$$\lambda_1(z_1, z_2) = \lambda_1^{(0)}(z_1, z_2) + r\lambda_1^{(1)}(z_1, z_2)$$
$$z_{1/2} = z_{1/2}^{(0)}(\rho) + r z_{1/2}^{(1)}(\rho)$$
$$J_1 = J_1^{(0)}(\rho) + r J_1^{(1)}(\rho) \tag{2.47}$$

where $\lambda_1(z_1, z_2)$ is the largest eigenvalue of C. We didn't look for higher order terms, which would imply taking larger matrices than 3×3.

We start with the leading order in which case we have to deal with a 2×2 matrix. The two eigenvalues of the matrix C are:

$$\lambda_{1/2}^{(0)} = \frac{1}{2} \left(1 + z_1 + z_2 \pm \sqrt{(1 + z_1 + z_2)^2 - 4z_1 z_2} \right) \tag{2.48}$$

Using Eqs.(2.32) and (2.35) we get:

$$z_{1/2}^{(0)}(\rho) = \frac{\rho(1 - \rho)}{(1 - 2\rho)^2} \tag{2.49}$$

Introducing the expression (2.49) in Eq.(2.48) we find the eigenvalues of the matrix C at a given density:

$$\lambda_1^{(0)}(z,z) = \left(\frac{1-\rho}{1-2\rho}\right)^2$$

$$\lambda_2^{(0)}(z,z) = \left(\frac{\rho}{1-2\rho}\right)^2 \tag{2.50}$$

Using now Eq.(2.39), we derive in zero-th order the expression of the inverse correlation length:

$$M = 2\log\left(\frac{1-\rho}{\rho}\right) \tag{2.51}$$

It is interesting to observe that the "mass" vanishes for the maximum value of the density ($\rho = 1/2$) and diverges at small densities. We can now use the expression of the partition function

$$Z_L^{\mu,\mu} = \left(\lambda_1^{(0)}\right)^L \tag{2.52}$$

and Eq.(2.41) to get the expression of the current:

$$J_1^{(0)} = \frac{\lambda\rho}{1-\rho} \tag{2.53}$$

To get the next order terms in r, we use the expression (2.46) for the matrix C and get the correction to the largest eigenvalue. We obtain:

$$\lambda_1^{(1)}(z_1,z_2) = \frac{\alpha\left(\lambda_1^{(0)}\right)^2 - \beta\lambda_1^{(0)} + \gamma}{3\left(\lambda_1^{(0)}\right)^3 - 2\delta\lambda_1^{(0)} + z_1 z_2} \tag{2.54}$$

where

$$\begin{aligned}
\alpha &= (1+2\lambda)(\delta - 1) \\
\beta &= (1+2\lambda)\delta(\delta - 1) - 2\lambda z_1 z_2 \\
\gamma &= ((1+\lambda)\delta - \lambda)\, z_1 z_2 \\
\delta &= 1 + z_1 + z_2
\end{aligned} \tag{2.55}$$

It is obvious how to proceed further. We get:

$$\lambda_1^{(1)}(z,z) = \rho^2 \frac{1 + 2\lambda - 2\rho - 2\lambda\rho}{(1-2\rho)^2}$$

$$z^{(1)} = -\rho^2 \frac{\lambda + (1 - 3\rho + \rho^2)(1+\lambda)}{(1-\rho)^2\,(2\rho^2 + 1 - 2\rho)} \tag{2.56}$$

$$J_1^{(1)} = -\rho^2\lambda \frac{1 + 2\lambda - \rho(6+9\lambda) + \rho^2(12+13\lambda) - \rho^3(6-2\lambda) - \rho^4(6+8\lambda) + 4\rho^5(1+\lambda)}{(1-\rho)^4\,(2\rho^2 + 1 - 2\rho)}$$

One interesting result that one can read from Eq.(2.56) is that, at fixed λ, the current reaches the asymptotic value for $q \to \infty$ from below.
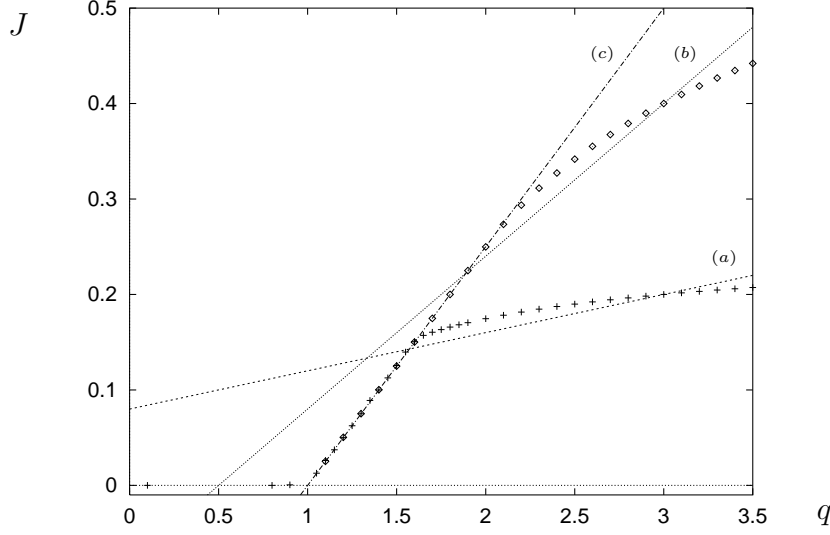
Figure 1. The current J as a function of q for $\lambda = 1$ and two densities ($\rho = 0.2$ (+) and $\rho = 0.4$ ($\diamond$)) The mean-field values are given by the dashed lines (a) ($\rho = 0.2$) and (b) ($\rho = 0.4$). The line (c) is given by Eq.(3.5). The data are the results of extrapolations using the grand canonical ensemble and L up to 200.

3. The currents.

From now on, the particles of type 1 and 2 will be called positive respectively negative because we think that it is easier to visualise the physics in this way. Their densities will be denoted by p respectively m (the density of vacancies will be v). If the densities of positive and negative particles are equal (this is going to be mostly the case), we will write

$$p = m = \rho . \tag{3.1}$$

It is useful to give the expression of the currents in the mean-field approximation. From Eq.(2.19) we get:

$$\begin{aligned} J_+ &= \lambda pv + (q - 1)pm \\ J_- &= \lambda mv + (q - 1)pm \end{aligned} \tag{3.2}$$

where obviously

$$p + m + v = 1 . \tag{3.3}$$

As is shown in Appendix B (see also Sec.6), the mean-field equations have not only homogeneous solutions. Here we refer to the homogeneous solutions. We will give first some pictures showing the q dependence of the currents at fixed values of λ and densities. These pictures are just a few from the data we collected. Our conclusions will be based

on all the available information. The thermodynamical limit for the values of the current have been obtained using the algebraic approach to the grand canonical ensemble (see Sec.2.3) up to $L = 200$. The large L limit has been obtained using extrapolants [14]. All the results have been checked using Monte-Carlo simulations (this corresponds to the canonical ensemble).

Since we consider the case in which the densities of positive and negative particles are the same and therefore one has:

$$J_+ = J_- = J \tag{3.4}$$

In Fig.1 we show the current for fixed $\lambda = 1$ and two values of the density ($\rho = 0.2$ and 0.4). The large q behavior of the current is not shown in the picture since its expression is known from Eq. (2.47). We distinguish three domains that for good reasons we are going to call phases. The names for the phases will look natural in the next sections.

a) *Pure phase* $(0 < q < 1)$ where the current is zero.

b) *Mixed phase* $(1 < q < q_c)$ where the current is given by
$$J = \frac{q-1}{4} \tag{3.5}$$
(see the line (c) in Fig.1), for both densities. The critical value of q denoted by q_c is density dependent.

c) *Disordered phase* $(q > q_c)$ where the current is density dependent. For large values of q, the current is given by the large q-expansion (see Eqs.(2.47), (2.53) and (2.56)).

The solid lines (a) and (b) in Fig.1 are the mean-field values obtained from Eq.(3.2). One can notice two facts. First, for $q = 3$ mean-field gives the current correctly. This should not come as a surprise since from Eq.(2.14) with $\lambda = 1$, we learn that the quadratic algebra has a one-dimensional representation, which implies that mean-field is exact. Next, we observe that, for both densities, mean-field gives correctly the currents for values of q close to q_c. This result has deeper consequences as will be seen in Sec.6, where it will be shown that at q_c the current is given by mean-field and that the discrepancy shown in Fig.1 comes probably from finite-size effects (one extrapolates from $L = 200$).

Having in mind Eq.(3.5), in Fig.2 we show the quantity $4J/(q-1)$ as a function q for fixed density ($\rho = 0.2$) and three values of λ. The same three phases are present. We notice that the current vanishes in the pure phase, that it is given by Eq.(3.5) in the mixed phase and that q_c increases with λ. For $\lambda = 0$ the current vanishes for any value of q (see Eq.(2.20)).

Similar calculations for other densities and values of λ have shown that in the pure phase the current vanishes and that in the mixed phase it is given by the simple expression (3.5) independent of density and λ. This is a very unexpected result. The values of q_c are dependent on λ and on the density. In Sec.6 we will derive the expressions of q_c (see Eq.(6.26) for equal densities) and the finite-size corrections. The interested
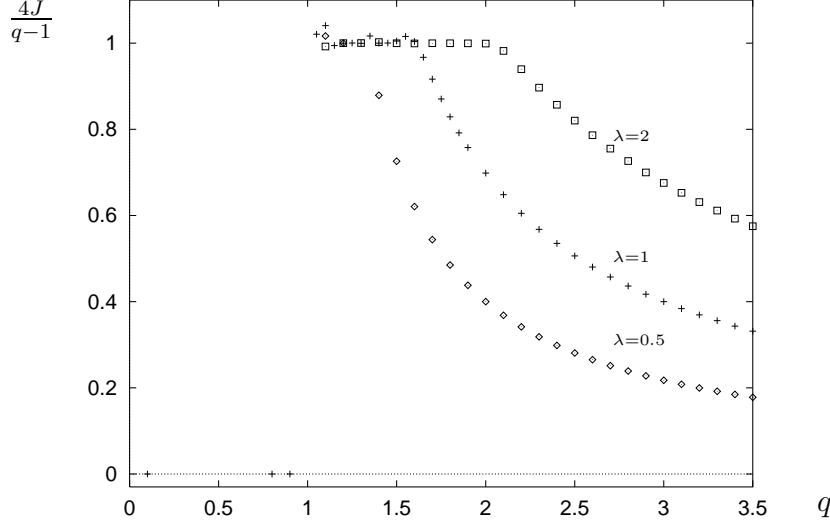
Figure 2. The q dependence of $4J/(q-1)$ for fixed $\rho = 0.2$ and three values of λ ($\lambda = 0.5, 1$ and 2). The data are obtained like in Fig. 1.
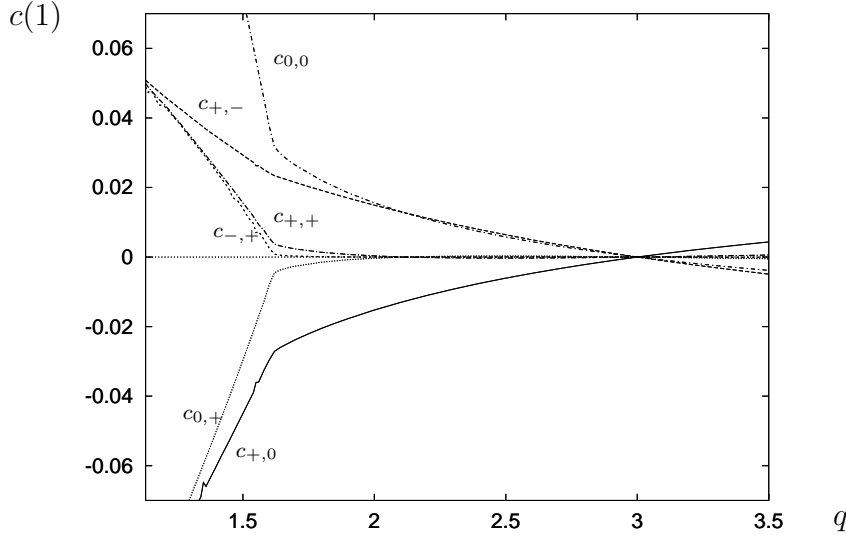

Figure 3. Large L limit of the connected nearest neighbour correlations $c_{+,0}(1) = c_{0,-}(1)$, $c_{0,+}(1) = c_{-,0}(1)$, $c_{-,+}(1)$, $c_{+,+}(1) = c_{-,-}(1)$, $c_{+,-}(1)$ and $c_{0,0}(1)$ for $\lambda = 1$ and $\rho = 0.2$. The data are the results of extrapolations using the grand canonical ensemble and L up to 150.

reader can already have a look at Fig.7 where the density dependence of the current is shown for various lattice sizes.

It is obvious from the Figs.1 and 2 that at q_c the derivative of the current has a discontinuity. In Fig.3 we show other local quantities, which are various connected correlations functions at distance 1 (one lattice site) for $\lambda = 1$ and $\rho = 0.2$. The

large L limit was obtained using the grand canonical ensemble extrapolating from data obtained up to $L = 150$. One notices that the derivatives of all these quantities have also a discontinuity at $q_c = 1.62$ (see Table 1). The Fig.3 shows also an interesting fact: for reasons which remain a mystery, the connected function $c_{-+}(1)$ practically vanishes in the disordered phase such that the discontinuity of its derivative is easier to determine. This allows the best estimate of $q_c = 1.62 \pm 0.04$.

In the next sections we are going to discuss at length the three phases. It is however very instructive to describe what one can see on the screen of the terminal while looking at the succession of configurations of a single Monte-Carlo run. This is of course a qualitative picture only. First, let us consider the pure phase. In order to fix the ideas, assume $q = 0.8$, $\lambda = 1$ and $\rho = 0.2$ (see Fig.1). For lattices lengths $L < L_1$ ($L_1 \approx 20$), one sees a uniform distribution of positive, negative particles and vacancies. For $L_1 < L < L_2$ ($L_2 \approx 30$) one observes a separation into two domains: one containing only positive and negative particles and one in which one has predominantly vacancies but also some charged particles. For $L > L_2$ one sees three domains one purely positive, one purely negative and one purely neutral (hence the name pure phase). These domains look like pinned in space (they move very slowly from one place on the ring to another one). In the mixed phase, (take $q = 1.2$, $\lambda = 1$, $\rho = 0.2$, see again Fig.1) the evolution with L of the relevant configurations is similar but by no means identical. Again for $L < L_1$ ($L_1 \approx 80$) the distributions are uniform, For $L_1 < L$ there is again a separation into two domains. In the first, one has only positive and negative particles with non-uniform distributions, we call it *condensate*. In the second domain, positive, negative particles and vacancies are uniformly distributed, we call this domain *fluid*. Increasing L, the concentrations inside the condensate change slowly and get more uniform and the fluid survives as a domain with a uniform distribution of the three species. This is one major difference between the pure and mixed phases. A second one comes from the observation that these profiles are not anymore pinned in the space but have a Brownian motion on the ring.

Before closing this section we would like to discuss the problem of finite-size corrections to the current.

It is amusing to start with a simple problem. Let us take $\lambda = 1$ and $q = 3$ and equal densities ρ. As already observed before, in this case one has a one-dimensional representation of the quadratic algebra (2.3) which can be obtained using Eq.(2.13):

$$G_0 = G_1 = G_2 = 1 \tag{3.6}$$

One can then do the calculations in the canonical ensemble where one gets in leading order
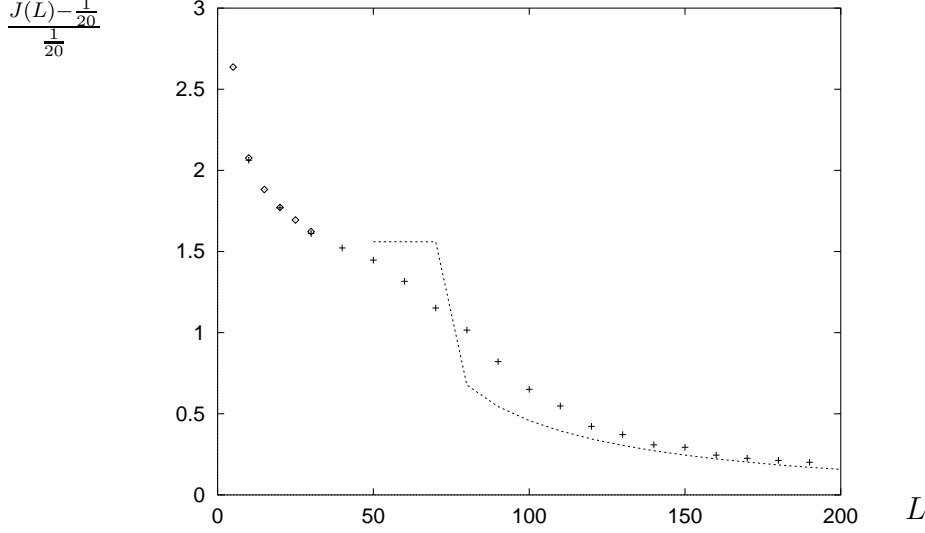
$$J = \rho(1 + \frac{1}{L}) \tag{3.7}$$

Figure 4. The deviation of the current $J(L)$ for L sites from its asymptotic value 0.05 in the canonical ensemble ($q = 1.2$, $\lambda = 1$, $\rho = 0.2$). The values obtained using Monte-Carlo simulations (+) are shown together with those using the algebraic approach ($\diamond$, up to $L = 30$) and with those from inhomogeneous mean-field solutions (dotted line) as described in Appendix B.

and in the grand canonical ensemble where one obtains

$$J = \rho \tag{3.8}$$

for any number of sites. This result is surprising since the parameters are such that we are in the disordered phase and one would expect exponential corrections (as will be shown in Sec.8 the correlation length is finite in this phase).

We have looked in several cases to the finite-size correction terms and the results are given below. All data are for $\lambda = 1$, $\rho = 0.2$. First we consider the grand canonical ensemble:

$$
\begin{array}{lll}
q = 0.8 & J = 0.09 \exp(-0.055L) & \text{(pure phase)} \\
q = 1.2 & J = 0.05 + 1.6/L & \text{(mixed phase)} \\
q = 2.2 & J = 0.18158 + 0.04/L^2 & \text{(disordered phase)} \\
q = 3.8 & J = 0.21065 - 0.016/L^2 & \text{(disordered phase)}
\end{array}
\tag{3.9}
$$

For the canonical ensemble, it is harder to estimate the correction terms. In order to illustrate the problem, we take $q = 1.2$ in the mixed phase. In Fig.4 we show the deviation of the current from its asymptotic value (0.05) as a function of the number of sites L. The Monte-Carlo data are shown together with the results obtained using the approach presented in Sec.2.2. Looking at the Monte-Carlo data first (up to $L = 200$) one observes that one gets large corrections. (The Monte-Carlo data are not precise
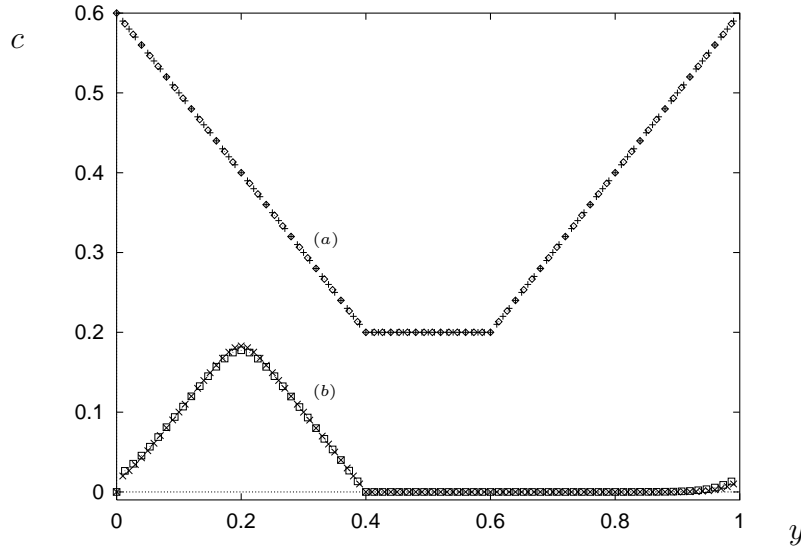
Figure 5. The y dependence of the two-point correlation functions $c_{0,0}$ (a), $c_{+,-}$ (b) in the pure phase ($q = 0.5$, $\lambda = 1$, $\rho = 0.2$) and lattice sizes $L = 75(\diamond, \square)$ and $L = 100(+, \times)$. (Monte-Carlo simulations).

enough to use extrapolants). On the other hand, the data obtained in the algebraic approach are in a range of L in which any extrapolation is bound to give wrong results. In Fig.4 we also show the values of the current obtained from the inhomogeneous solutions of the mean-field equations (see Appendix B). At large values of L the current obtained in this way is in agreement with the Monte-Carlo data, but at small values of L, they show a curious behavior. The explanation of this phenomenon and a more extensive discussion of the finite-size corrections in the mixed phase for the canonical ensemble can be found in Sec.6. There is a case in which the finite-size corrections converge very nicely. This is the case $q = 1$. Moreover, in Sec.6 we will even show how to get them theoretically. Here, we just give the Monte-Carlo results, again for $\lambda = 1$ but for different densities:

$$
\begin{aligned}
\rho &= 0.1 & J &= 5/L \\
\rho &= 0.2 & J &= 2.5/L \\
\rho &= 0.4 & J &= 1.25/L
\end{aligned}
\tag{3.10}
$$

The reader can easily guess the analytical expression of the correction term. In order to help the reader, we have not given the errors in Eq. (3.10) (they are small).

We will now discuss in detail the three phases.

4.   The pure phase $(0 < q < 1)$

In the last section we have mentioned that in the pure phase the current vanishes exponentially with the lattice size for any values of the densities (they might be different) and of λ. We will now get a complete picture of this phase (it is very simple).

At $q = 0$, a single vacancy is sufficient to break the translational invariance of the system. At a finite density of vacancies, the ground state of the time evolution hamilton operator is infinitely degenerate for $L = \infty$, each configuration of the kind

$$(0) \cdots (0)(+) \cdots (+)(-) \cdots (-)(0) \cdots (0)(+) \cdots (+)(-) \cdots (-) \cdots \qquad (4.1)$$

being a stationary state. At q different from zero and finite L, if one starts with an arbitrary configuration, the system organizes itself into only three blocks

$$(0) \cdots (0)(+) \cdots (+)(-) \cdots (-) \qquad (4.2)$$

which cover the lattice. Translational invariance is respected but as shown in Sec.7 the blocks hop from one position to another with a flip time which increases exponentially with L. This implies that for $q < 1$, translational invariance is spontaneously broken. Since each of the three blocks contains one kind of particle only, we call it the pure phase.

We postpone the discussion of the flip times and of the behavior of the order-parameter which describes the breaking of translational invariance. This is going to be done in Sec.7 in conjunction with a similar problem but with different results for the mixed phase.

In Fig.5 we show the two-point correlation functions $c_{0,0}$ and $c_{+,-}$ defined by Eq.(2.37) not as a function of the distance R measured in lattice sites but of the macroscopic distance

$$y = R/L \qquad (4.3)$$

For any fixed y, the data converge exponentially to their thermodynamic limit. This explains why the correlations functions for so small lattices ($L = 75$ and 100) coincide already. The expression of the correlation functions for very small lattices can be derived from the mean-field calculations presented in Sec.6. It was checked using Monte-Carlo simulations that these calculations give the correct picture of finite-size effects.

We invite the reader to compute the two-point functions using the three blocks picture (4.2) and he will discover that he will get precisely the results presented in Fig.5. This applies also to the other two-point functions. Obviously, the correlation functions dependent only on the densities but not on λ.

That in the pure phase one has charge segregation is obvious. Not only the correlation functions do depend on y in agreement with the definition given in Sec.1, but the configurations described by (4.2) give the simplest example of segregation. The mixed phase will provide another example.
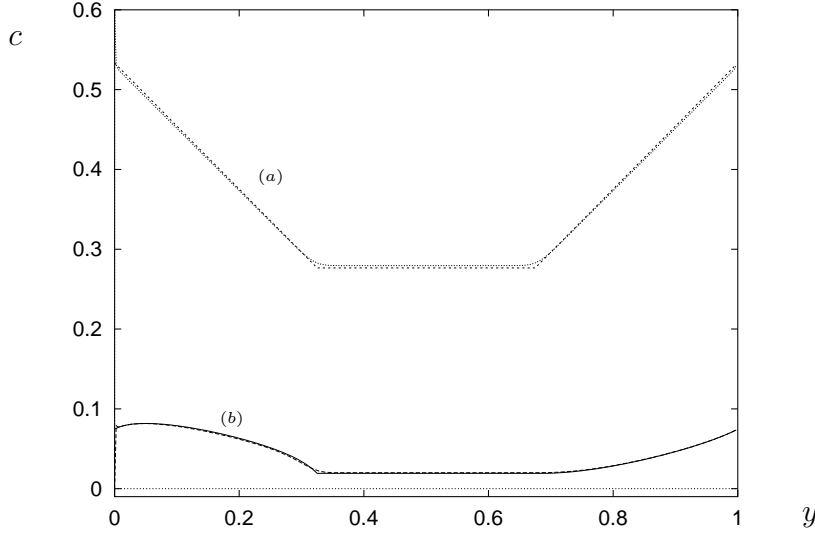
5. The mixed phase $(1 < q < q_c)$

Figure 6. The correlation functions $c_{0,0}$ (a) and $c_{+,-}$ (b) obtained from Monte-Carlo simulations for $\rho = 0.2$, $q = 1.2$, $\lambda = 1$, and $L = 400$. The solid lines are obtained using the mean-field results presented in Sec.6.

In Sec.3 we have seen that in the mixed phase, for any ρ and λ, the current is given by the expression (3.5). We are going to analyse this phase in more detail. In Figure 6 we show for $q = 1.2$, $\lambda = 1$ and $\rho = 0.2$ (one can check from Fig.1 that we are in the mixed phase) the correlation functions $c_{0,0}$ and $c_{+,-}$ as a function of y for $L = 400$. The "macroscopic" variable y is defined in Eq.(4.3). The correlation functions were obtained using Monte-Carlo simulations. As will be explained in Sec.9 one can't use the grand canonical ensemble to compute correlation functions for large distances (this is not the case for the current) in the mixed or pure phases but only in the disordered phase.

It is interesting to compare the correlation functions in the mixed phase and in the pure phase (see Fig.5). They look similar. The $c_{0,0}$ function has the same shape in both cases although the values of $c_{0,0}$ are different. For example the widths of the plateau have different values. The $c_{+,-}$ functions have a slightly different shape (compare the behaviors for $y < 0.4$ and $y > 0.7$). One could be tempted to conclude that there are no major differences between the two phases. This is not the case. As we mentioned, in the pure phase the data presented in Fig.5 represent already the thermodynamical limit. The data presented in Fig.6 although obtained for a large lattice do not represent the thermodynamical limit. There is a slow change with L of the behavior of the correlation

functions not shown in the figures. We took data for lattice sizes up to $L = 800$, the L dependence is well taken into account by the mean-field calculations presented in the next section. That these mean-field calculations make sense can already be seen in Fig.6 where the solid curves which are on top of the Monte-Carlo data are mean-field results. After presenting the mean-field results we are going to compare them with other data obtained from Monte-Carlo simulations (see Figs.8 and 9).

At this point the reader should accept the fact that the correlation functions converge at large L to non-trivial functions of y (this is going to be explained in the next section) and therefore in the mixed phase, like in the pure phase we have charge segregation.

As we are going to prove in Sec.7 the major difference between the two phases is that, as opposed to the pure phase, in the mixed phase translational invariance symmetry is not spontaneously broken.

6. Inhomogeneous solutions of the mean-field equations. The pure and mixed phases.

We have postponed the presentation of mean-field for the following reason. We had first to present the empirical data for the correlation functions in order to know how the mean-field calculations have to be done. Since for a given lattice size L, the correlation functions depend smoothly on the "macroscopic" variable y ($0 < y < 1$), this suggests to work in the continuum taking y as variable and L as a parameter in the mean-field equations. The previous mean-field calculations in similar problems (see for example Refs. [16] and [17]) were done in a different way. The mean-field equations for the stationary state are a couple of non-linear differential equations and it is not clear a priori how to solve them. The inspiration came from getting, numerically, the solutions on small lattices. The results of these investigations as well the mean-field equations in the continuum are presented in Appendix B. About the relevance of mean-field to our problem, we are going to comment later.

In Appendix B it is shown that the for given values of q, λ and densities in the pure or mixed phases the mean-field equations on the lattice have besides an homogeneous solution (which was used in Eq.(3.2)) inhomogeneous ones. These solutions are "pinned" in space even for a finite lattice. Otherwise speaking, in mean-field translational invariance is broken in both the pure and mixed phases. These conclusions are based on numerical results. One remarkable property of the inhomogeneous solution (see Figs.B1 and B2) is that it shows two domains one with charged particles only (we called it condensate) and one with charged particles and vacancies (we called it fluid). In this section we are going to present the stationary solutions of the mean-field equations (B.3–B.6) which we were able to obtain by making the Ansatz of the existence of a condensate and a fluid. A stationary non-homogeneous solution of the mean-field equations will be

contain at least one bump. In the present paper we consider the solutions with one bump only since they are relevant for our problem. Solutions with more bumps are shortly mentioned in Appendix B and discussed in detail in [7]. These solutions always breaks translational invariance. We will assume that mean-field gives the correct description of our physical problem (we will return to this point at the end of this section) if its solutions are used in different ways for the pure and mixed phases.

We will work with "macroscopic" variables like in equation (4.3). In this case the ring has a perimeter of length 1. For the mixed phase we will assume that with equal probability for each point z on the ring ($0 < z < 1$) one has a bump which contains a condensate of length a and a fluid of length b (this implies that one has translational invariance) and that mean-field describes both of them. For the pure phase we take the results of mean-field at face value: the bump is "pinned" in space and translational invariance is broken. In both phases the values of a and b are L-dependent and their values in the thermodynamical limit will be denoted by A and B. Obviously

$$a + b = 1 \ . \tag{6.1}$$

It is convenient to choose a coordinate y with the origin at the beginning of the condensate. Thus, if $0 < y < a$ we are in the condensate, and if $a < y < 1$ we are in the fluid. The names condensate and fluid are naturally related to Bose-Einstein condensation. As will be shown in Sec.9 a similar phenomenon takes place in our system. We assume that there are no correlations in the condensate and the fluid so that we can apply mean-field theory. The present calculation will give not only the concentrations of particles but also the values of the current and the length b of the fluid as a function of L. We start with the fluid and assume that on the segment of length b the concentrations of positive and negative particles, $\rho_+^{\mathrm{fl}}(L)$ and $\rho_-^{\mathrm{fl}}(L)$, and implicitly of vacancies, $\rho_0^{\mathrm{fl}}(L)$, are independent of y but L dependent. One has:

$$\rho_+^{\mathrm{fl}}(L) + \rho_-^{\mathrm{fl}}(L) + \rho_0^{\mathrm{fl}}(L) = 1 \tag{6.2}$$

In the condensate, one has no vacancies, the concentrations of positive and negative particles ($\rho_+^{\mathrm{co}}(y, L)$ and $\rho_-^{\mathrm{co}}(y, L)$) are y and L dependent and satisfy the relation:

$$\rho_+^{\mathrm{co}}(y, L) + \rho_-^{\mathrm{co}}(y, L) = 1 \tag{6.3}$$

We will consider three cases. We take the same density of positive and negative particles

$$\rho = \frac{1 - v}{2} \tag{6.4}$$

and q greater than 1, next $q = 1$ and $q < 1$. Various predictions obtained from mean-field will be compared with the results obtained from Monte-Carlo simulations.
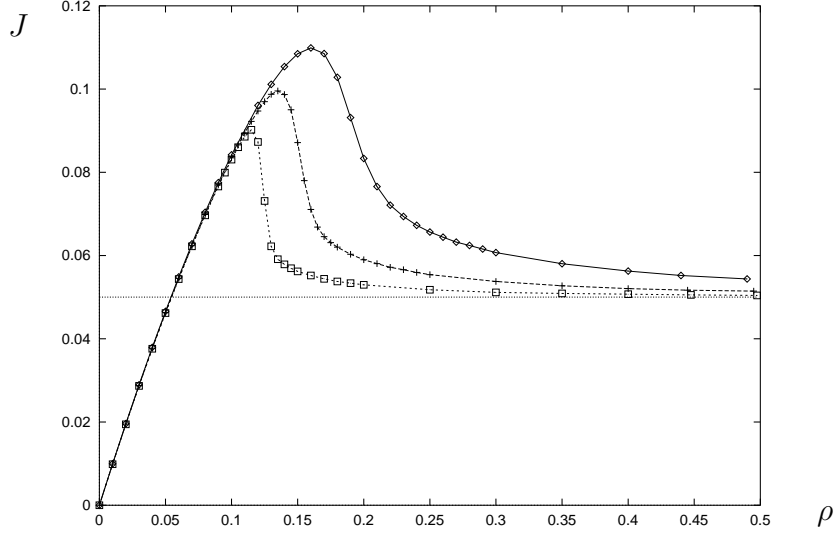
Figure 7. The current as a function of the density. The data are obtained from Monte-Carlo simulations for $q = 1.2$ and $\lambda = 1$ and $L = 100$ (top), $L = 200$ and $L = 400$ (bottom). The horizontal line gives the value of the current in the mixed phase (see Eq.(3.5)).

6.1. $q > 1$ (mixed phase)

6.1.1. Profiles for finite L In the fluid we have

$$\rho_+^{\text{fl}} = \rho_-^{\text{fl}} = \frac{1}{2}(1 - \rho_0^{\text{fl}}) \tag{6.5}$$

and

$$b\rho_0^{\text{fl}} = v \tag{6.6}$$

The current is

$$J = \lambda \rho_+^{\text{fl}} \rho_0^{\text{fl}} + (q - 1)\rho_+^{\text{fl}} \rho_-^{\text{fl}} \tag{6.7}$$

For later convenience, it is useful to define

$$\alpha = \sqrt{\frac{4J}{q - 1} - 1} \tag{6.8}$$

It is clear that if the current has the expression (3.5), this implies $\alpha = 0$ and that non-zero values for α give finite-size corrections. Using Eqs.(6.5)-(6.8) we get:

$$\alpha^2 = \frac{v}{b(q - 1)}\left(2(\lambda + 1 - q) + \frac{v}{b}(q - 1 - 2\lambda)\right) \tag{6.9}$$

We define

$$B = \frac{v(1 - q + 2\lambda)}{2(1 - q + \lambda)} . \tag{6.10}$$

As will be seen, B will represent the large L limit of the length b of the fluid. Denoting

$$\gamma = \frac{v}{B} - \frac{v}{b} \tag{6.11}$$

and using Eq.(6.9) we obtain

$$\alpha^2 = \frac{2(1 + \lambda - q)}{q - 1}\gamma \left(1 - \frac{1 - q + 2\lambda}{2(1 - q + \lambda)}\gamma\right) . \tag{6.12}$$

Eq.(6.12) connects the value of the current and the width of the fluid. We are going to obtain a second equation relating the same quantities examining the condensate. We write the expression of the current in the condensate in the mean-field approximation in a symmetric way

$$\begin{aligned}
J &= \frac{q}{2}\left(\rho_+^{co}(y - \frac{1}{L})\rho_-^{co}(y) + \rho_+^{co}(y)\rho_-^{co}(y + \frac{1}{L})\right) \\
&\quad - \frac{1}{2}\left(\rho_-^{co}(y - \frac{1}{L})\rho_+^{co}(y) + \rho_-^{co}(y)\rho_+^{co}(y + \frac{1}{L})\right)
\end{aligned} \tag{6.13}$$

and define

$$\rho_\pm^{co} = \frac{1}{2} \pm w . \tag{6.14}$$

Eq.(6.3) is then satisfied for any w. Using Eqs.(6.13) and (6.14) and going to the continuum limit we find the following expression for the current:

$$J = (q - 1)(\frac{1}{4} - w^2) - \frac{q + 1}{2L}\frac{dw}{dy} \tag{6.15}$$

(an analogous expression for the current appeared for the first time in Ref. [18]) The same relation could have been obtained directly from Eq.(B.3) We keep in mind that charge conservation gives

$$\int_0^a \rho_\pm^{co}\,dy = \frac{a}{2} . \tag{6.16}$$

We will now impose boundary conditions for the differential equation (6.15). We will require that the concentration of positive particles is continuous at the end of the condensate $(y = a)$ and that of the negative particles at the beginning of the condensate $(y = 0)$:

$$\begin{aligned}
\rho_+^{co}(a) &= \rho_+^{fl} \\
\rho_-^{co}(0) &= \rho_-^{fl}
\end{aligned} \tag{6.17}$$

Notice that in this way, the density of positive particles $\rho_+(y)$ is continuous at the point a but discontinuous in the origin where one has a shock even at finite L. Conversely,

the density of negative particles $\rho_-(y)$ is continuous for $y = 0$ but not for $y = a$. Using Eq.(6.15) and (6.17) we get the profile of the concentrations in the condensate:

$$w = \frac{\alpha}{2}\tan\left(\beta(\frac{a}{2} - y)\right) \tag{6.18}$$

where α is given by Eq.(6.8), and β is related to α:

$$\beta = \frac{q-1}{q+1}L\alpha \tag{6.19}$$

The boundary conditions give:

$$\beta\tan(\frac{\beta a}{2}) = \frac{q-1}{q+1}\frac{v}{1-a}L \tag{6.20}$$

The equation (6.20) relates again the current to the width of the fluid. In this way, from the Eqs.(6.12) and (6.20) we can derive both the current J and b as functions of v, λ, q and L. Once they are known, using (6.6) and (6.18) one can derive the concentrations in the condensate and the fluid. Knowing the concentrations, one can compute any correlation function like $c_{0,0}$, $c_{+,-}$, etc.

Notice that for $y = 0$ the density ρ_+ is discontinuous even for finite L. Therefore the bump ends with a shock on the left. As we are going to show shortly the bump will end with a shock also on the right in the large L limit.

In order to solve the transcendental equations (6.12) and (6.20), we will do a large L expansion. It is convenient to define a new variable u instead of β:

$$\beta = \frac{\pi - 2u}{a} \tag{6.21}$$

and instead of Eq.(6.20) we obtain:

$$\frac{\tan u}{1 - \frac{2u}{\pi}} = \delta(1-a)v^{-1} \tag{6.22}$$

where

$$\delta = \frac{\pi(q+1)}{La(q-1)}. \tag{6.23}$$

Keeping only the term of order u in the left-hand side of Eq.(6.22) and using Eqs. (6.19) and (6.21) we obtain:

$$\alpha^2 = \delta^2(1 - \frac{4(1-a)}{v\pi}\delta) \tag{6.24}$$

We now use Eq.(6.12) to obtain:

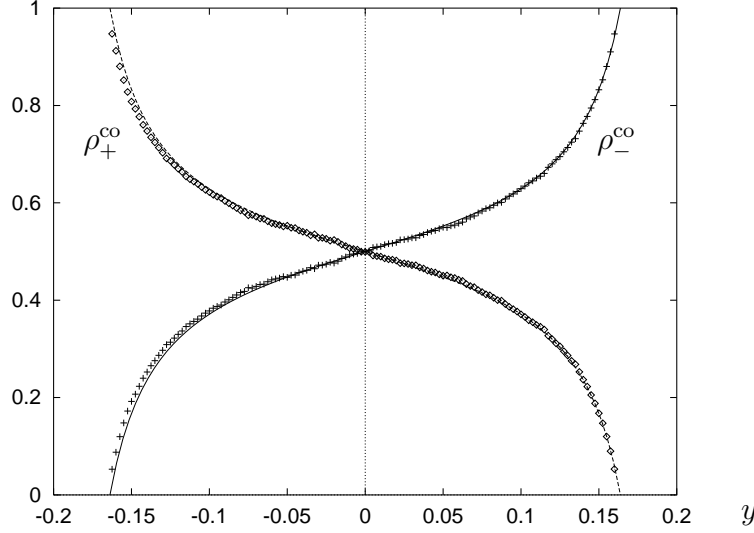$$\gamma = \frac{\delta^2(q-1)}{2(1 + \lambda - q)} \tag{6.25}$$

Figure 8. The concentrations of positive and negative particles in a shock ($q = 1.2$, $\lambda = 1$, $\rho = 0.2$, $L = 400$) obtained from Monte-Carlo simulations and from the model as described in the text (solid curves).

Collecting all the results together, we obtain finally:

$$\frac{4J}{q-1} = 1 + \left(\frac{(q+1)\pi}{(q-1)AL}\right)^2 \left(1 - \frac{4(q+1)(1-A)}{L(q-1)vA}\right) \tag{6.26}$$

and

$$\frac{b-B}{v} = \left(\frac{B}{v}\right)^2 \frac{(q+1)^2\pi^2}{2(1+\lambda-q)(q-1)A^2L^2} \tag{6.27}$$

where

$$A = 1 - B. \tag{6.28}$$

B is the length of the fluid in the thermodynamic limit and A is the length of the condensate. From Eq.(6.26) we learn that in the large L limit the current is indeed given by Eq.(3.5) and that the finite-size correction terms are not only q dependent but (through A) are dependent also on the density of vacancies v and on λ. Notice that the finite-size corrections to the current although quadratic in $1/L$ (the relevant parameter is δ given by Eq.(6.23)) can be large even for large lattices, say $L = 200$. We remind the reader that in Sec.3 we have shown that in the grand canonical ensemble the finite-size corrections are linear in $1/L$. A different finite-size behavior for the two ensembles was already noticed for the disordered phase (see Eqs.(3.7-10)).

6.1.2.   Comparison of the mean-field predictions with results obtained by other methods. Finite-size scaling.   We are now in the position to compare the result of the model
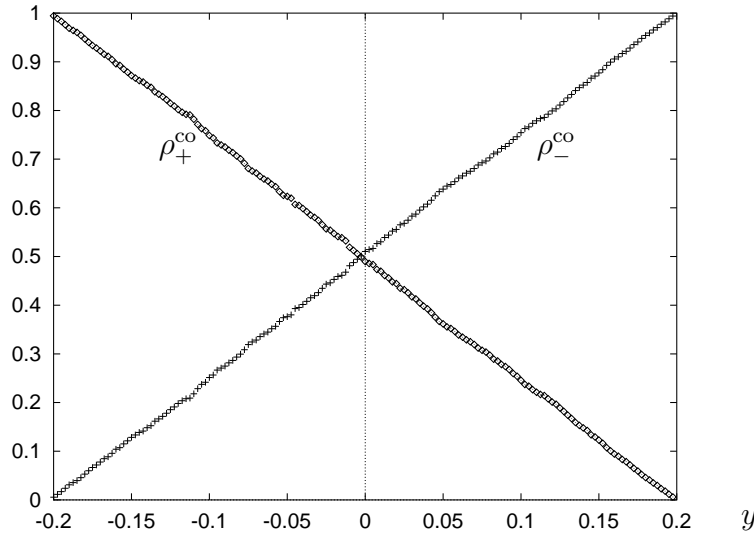
Figure 9. Like in Fig.8 except that here $q = 1$.

with the Monte- Carlo data. We first start with the current (see Fig.4). We notice that for large values of L $(L > 150)$ the mean-field values obtained using the method of Appendix B which are already almost identical with those obtained in the continuum approximation given above are close to the Monte-Carlo data. One can be more precise: Using Eq.(6.26) with $q = 1.2\,\lambda = 1\,\rho = 0.2$ one gets $J = 0.0534$ for $L = 200$ and $J = 0.0522$ for $L = 400$ to be compared with the values $J = 0.059$ respectively $J = 0.053$. This observation is interesting since one wouldn't expect a mean-field calculation to control so well finite-size corrections. For smaller values of L (see again Fig.4), the Monte-Carlo data (confirmed by the calculations done using the algebraic approach) as well as the mean-field values show a strange behavior of the current in the region $50 < L < 70$. The explanation of this phenomenon is simple. For given values of the parameters q, λ and ρ for which in the thermodynamical limit one is in the mixed phase, the bump picture appears only if the size L of the system is larger than a certain minimal value. We would like to add that we have not checked for which values of L the continuum version of mean-field coincides with the discrete version presented in Appendix B.

The phase diagram is at this point known. The mixed phase, for a given values of λ and ρ, is between $1 < q < q_c$, where q_c is

$$q_c = 1 + \frac{2\lambda(1 - v)}{2 - v}. \tag{6.29}$$

This value is obtained from the condition

$$B = 1 \tag{6.30}$$

which says that one has no condensate.

Table 1. The estimates of the critical value of q obtained using the grand canonical ensemble (q_c^{gc}) or Monte-Carlo simulations (q_c^c) compared with the values q_c given by formula (6.29).

	$p = m = 0.1$		$p = m = 0.2$		$p = m = 0.4$	
λ	q_c^{gc}	q_c	q_c^{gc}	q_c	q_c^{gc}	q_c
0.25	1.10	1.08	1.2	1.14	1.3	1.22
0.50	1.15	1.17	1.3	1.29	1.6	1.44
0.75	1.25	1.25	1.5	1.42	1.8	1.67
1.00	1.35	1.33	1.62	1.57	2.2	1.89
2.00	1.60	1.67	2.2	2.14	2.9	2.78
3.00	1.85	2.00	2.5	2.71	3.5	3.67
4.00	2.0	2.33	2.8	3.28	3.8	4.56

One can ask to which extent the mean-field prediction (6.29) is correct. In Table 1 we present the estimates of the critical points q_c^{gc} obtained from the "discontinuities" of the derivatives of the current and of the two-point functions $c_{-,+}(1)$ as a function of q using the grand canonical ensemble (see Sec.3) together with the values of q_c obtained using formula (6.29). The estimates have errors which are hard to evaluate, therefore an optimistic point of view would suggest that (6.29) is exact. A pessimist would say that mean-field is a good approximation in the vicinity of the phase transition only for low values of λ and densities. An argument in favor of the optimistic point of view will be given below.

A well known question in equilibrium statistical physics is the problem of finite-size scaling corrections in the determination of critical points [19]. One can ask a similar question here. For a finite value of L (at fixed λ and ρ) an estimate of q_c can be obtained for example using the fact that in the thermodynamical limit the derivative of the current has a a jump at q_c which at finite values of L gives an obvious way to get an estimate for q_c. We would like to know how the estimate approaches q_c. In order to get an insight to this problem, one can assume that the current changes when the condensate appears. Therefore let us go back to Eq.(6.27) which gives the length of the condensate for finite L. One sees that $b > B$. In particular, for a given value of L, there is a value of q that we denote by $\tilde{q}_c(L)$ for which there is no condensate, i.e.

$$b(L) = 1 \,. \tag{6.31}$$

Denoting

$$\tilde{q}_c(L) = q_c - \epsilon \tag{6.32}$$

and using Eqs.(6.27) and (6.31) we obtain:

$$\epsilon^3 L^2 = \frac{8\lambda v\pi^2}{(2-v)^6(1-v)}(2-v+\lambda(1-v))^2 \tag{6.33}$$

From Eq.(6.33) we see that $\epsilon > 0$, which means that for a given value of $q < q_c$ up to a certain length L, one has no bump, in agreement with the interpretation given above to the behavior of the current as a function of L in Fig.4. On the other hand Eq.(6.33) gives obviously a finite-size scaling critical exponent $2/3$. Unfortunately, this derivation is only heuristic. Here are the reasons. A careful examination of the Eqs.(6.18–6.20) shows that the value $b(L) = 1$ is never obtained although the large L approximation (6.27) gives it. Mean-field theory suggests that the condensation appears directly with a non-zero value of the length a and implicitly a value of $b < 1$. Using this value of b (which is obtained from a transcendental equation) one can estimate numerically the critical exponent. It is also $2/3$ but the right hand side of Eq.(6.33) is different.

A careful examination of the Monte-Carlo data shows a similar phenomenon although the value of a at which the condensate appears is slightly different than the one predicted by mean-field.

Instead of working at fixed v and λ, one can take fixed q, λ (in the mixed phase) and L and look for at which density $\bar{v}_c(L)$ starts the condensation ($b(L) = 1$). We use again Eq.(6.27) and get

$$L^2\left(1 - \frac{\bar{v}_c(L)}{v_c}\right)^3 = \pi^2\frac{(q+1)^2}{(q-1)(1-q+2\lambda)} \tag{6.34}$$

where v_c is obtained from Eq.(6.10) with $B = 1$:

$$v_c = \frac{2(1-q+\lambda)}{1-q+2\lambda} \tag{6.35}$$

From Eq.(6.34) we learn that for finite L the condensation occurs at a lower density of vacancies (larger density of particles) than at the critical point. This behavior can also be seen in Fig.7 where the ρ dependence of the current at fixed $q = 1.2$ and $\lambda = 1$ is shown for various lattice sizes. For large values of ρ one is in the mixed phase ($J = (q-1)/4$). If we decrease the value of ρ the current increases (see Eq.(6.26)) up to a point where the condensate disappears. For small values of the density the mean-field approximation does not apply (one is in the disordered phase). If one increases the size of the lattice, the minimal value of ρ where mean-field still applies gets smaller and the current gets closer to its asymptotic value $(q-1)/4$. One way to estimate v_c is to take the values of the density $\bar{\rho}_c$ where the current has a maximum. One can then estimate the exponent alpha from the expression

$$1 - \frac{\bar{v}_c(L)}{v_c} = \text{const.}L^{-\alpha} \tag{6.36}$$

Using data taken at $L = 100, 200, 400, 800$ and 1600 one gets $\alpha = 0.5 \pm 0.2$ which makes the exponent $\alpha = 2/3$ given by Eq.(6.34) plausible. Moreover, this also implies that the mean-field value for v_c given by Eq.(6.35) is probably correct. The estimate of α has large errors since it is difficult to determine precisely the position of the maximum of the current.

We are going to verify the mean-field predictions in the mixed phase away from q_c. We take again $q = 1.2$, $\lambda = 1$, $\rho = 0.2$ and $L = 400$. Solving Eqs.(6.12) and (6.20) numerically and using Eqs.(6.18) and (6.19) we get:

$$J = 0.05257, \quad a = 0.3200, \quad w = 0.1134 \tan\left(8.244(\frac{a}{2} - y)\right) \tag{6.37}$$

We have done Monte-Carlo simulations taking only configurations in which a had approximately the value given in (6.37). For these configurations we have determined the concentrations of positive and negative particles. They are shown in Fig.8 together with the prediction obtained from Eq.(6.37). The agreement couldn't be better. One can use (6.37) in order to compute the correlation functions $c_{0,0}$ and $c_{+,-}$ and compare them with the Monte-Carlo data. This comparison can be seen in Fig.6 and was repeated for all correlation functions. The agreement is as good as for $c_{0,+}$ and $c_{-,+}$.

6.1.3. Profiles for large L We would like to discuss now the composition of the bump in the thermodynamical limit. We denote the concentrations by R instead of ρ. From Eqs.(6.14), (6.24) and (6.17), we get

$$R_\pm^{co}(y) = \frac{1}{2}, \qquad R_0^{fl} = \frac{v}{B}, \qquad R_\pm^{fl} = \frac{1 - R_0^{fl}}{2} \tag{6.38}$$

This result is mostly interesting. One can see the closed system as two open systems, one containing only positive and negative particles (the condensate) with equal concentrations and a second one containing also vacancies (the fluid). From our knowledge of the two-state model [1] with the bulk rates $g_{+,-} = q$, $g_{-,+} = 1$ we know that the current has the expression (3.5) from mean-field (it is just a repetition of the calculation done above where Eq.(6.17) is replaced by an equation which takes into account the boundary rates). This is the so-called maximum-current phase [3, 2]. In the same maximum-current phase but only for the case of totally asymmetric diffusion it was shown that the correlation functions have an algebraic decay. It is plausible to assume that the same applies for the partially asymmetric case which is ours. This would also suggest that the fluid phase is also algebraic. This assumption can be checked independently since the algebraic tools for this problem are already known [20]. Unfortunately we were not able to check if indeed the correlation functions $c_{0,0}$, $c_{+,-}$ etc. in the present model have an algebraic decay. This would imply to work not with the macroscopic variable y but with R (see Eq.(4.3)) and to take lattice sizes beyond our means.

The reader might have noticed that all the expansions used above diverge for $q = 1$ (see Eq.(6.23)). We proceed now to discuss this case.

6.2. $q = 1$

A repetition of the calculation done for the case $q = 1$ gives the following results. The current in the fluid phase has the expression:

$$J = \frac{\lambda}{2}(1 - \frac{v}{b})\frac{v}{b} \tag{6.39}$$

In the condensate, the current is

$$J = -\frac{1}{L}\frac{dw}{dy} \tag{6.40}$$

which can be obtained from Eq.(6.15) for $q = 1$. Taking into account the boundary conditions, we obtain:

$$w = \frac{v}{ab}(\frac{a}{2} - y) \tag{6.41}$$

and

$$J = \frac{v}{abL} \tag{6.42}$$

Equating the two expressions for the current (6.39) and (6.42), we find b as a function of L and consequently, J as a function of L. In order to show how good our results are, one can compare for $\lambda = 1$, $\rho = 0.2$ and $L = 100$ (which is a small lattice) the value of the current obtained using (6.39)-(6.42) which is $J = 0.02588$ with the Monte-Carlo value $J = 0.0256$.

In Fig.9, we compare the profiles, now for $q = 1$, just as we did in Fig.8 for $q > 1$. Notice the nice straight lines.

For large values of L one obtains the following leading contributions to the current

$$J = \frac{1}{(1 - v)L} - \frac{2(1 - 2v)}{\lambda(1 - v)^3 L^2} \tag{6.43}$$

and to the length of the fluid

$$b = v\left(1 + \frac{2}{\lambda L(1 - v)}\right) \tag{6.44}$$

which explains Eq.(3.10).

In the thermodynamic limit, keeping the notations used already, we get:

$$B = v, \qquad A = 1 - v \tag{6.45}$$

$$R_+^{fl} = 0, \qquad R_+^{co} = 1 - \frac{y}{A} \tag{6.46}$$

$$R_-^{fl} = 0, \qquad R_+^{co} = \frac{y}{A} \tag{6.47}$$

and of course $J = 0$.

It should be interesting to study in detail the properties of the fluid and the condensate at $q = 1$ looking not at macroscopic distances (y) but at microscopic ones (R).

6.3. $q < 1$ (pure phase)

One can repeat the calculations done for the mixed phase for the pure phase. We give directly the results. Instead of Eq.(6.18) one has:

$$w(y) = \frac{1}{2}\left(\frac{4J}{1-q}+1\right)^{1/2}\tanh\left(\frac{q-1}{q+1}L\left(\frac{4J}{1-q}+1\right)^{1/2}(\frac{a}{2}-y)\right) \quad (6.48)$$

which gives the profiles of the concentrations in the condensate, the boundary condition (6.20) been replaced by

$$w(0) = \rho_0^{\text{fl}} = v/b \quad (6.49)$$

This allows to obtain for large values of L the expression of the current:

$$J = \frac{\lambda(1-q)}{\lambda+1-q}\exp\left(\frac{q-1}{q+1}L(1-v)\right) \quad (6.50)$$

and of the density of vacancies in the fluid:

$$\rho_0^{\text{fl}} = 1 - 2J/\lambda \quad (6.51)$$

the last expression shows, as expected, that in the large L limit, the densities of vacancies in the fluid tends exponentially to 1 which is precisely what one expects in the fluid phase. The expression of the current given by Eq.(6.50) is compatible with the fits done to the Monte-Carlo data (see for example (3.9)). An exponential fall-off of the current was also observed in a different model [21].

7. The spontaneous breaking of translational invariance. Flip times in the pure and mixed phase

In the last sections we have described the pure and the mixed phases. Both phases show long range correlations which are different from a quantitative point of view (exponential versus algebraic finite-size convergence etc.), but up to this point we haven't proven that they are also qualitatively different. Moreover, mean-field calculations (see Appendix B and Sec.6) show no qualitative differences between the two phases: one obtains pinned configurations in both cases. We are going to show now that half of these mean-field predictions are wrong and that in the pure phase translational invariance is broken and that this is not the case for the mixed phase.
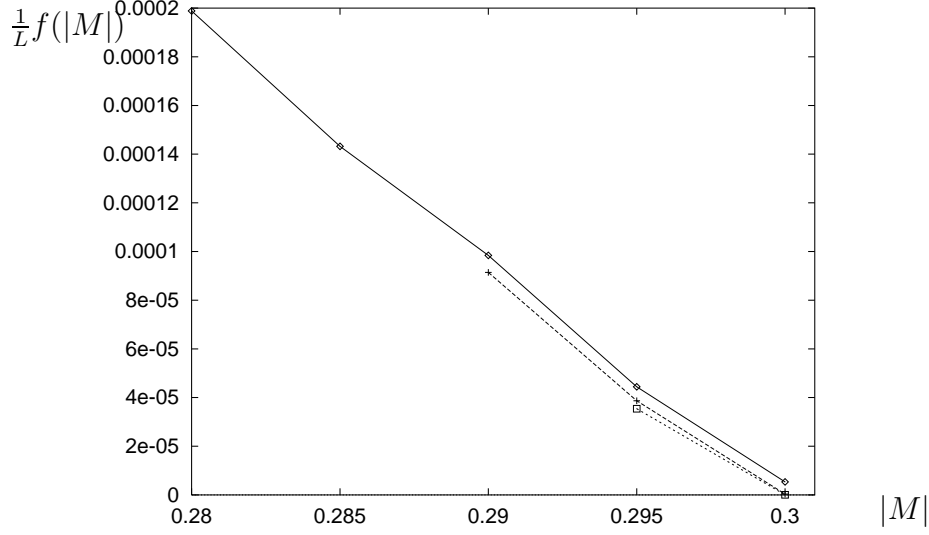
Figure 10. The Ginzburg-Landau potential in the pure phase ($\rho = 0.2$, $\lambda = 1$, $q = 0.9$) as a function of $|M|$ obtained from Monte-Carlo simulations for $L = 100(\diamond)$, $200(+)$ and $400(\square)$.
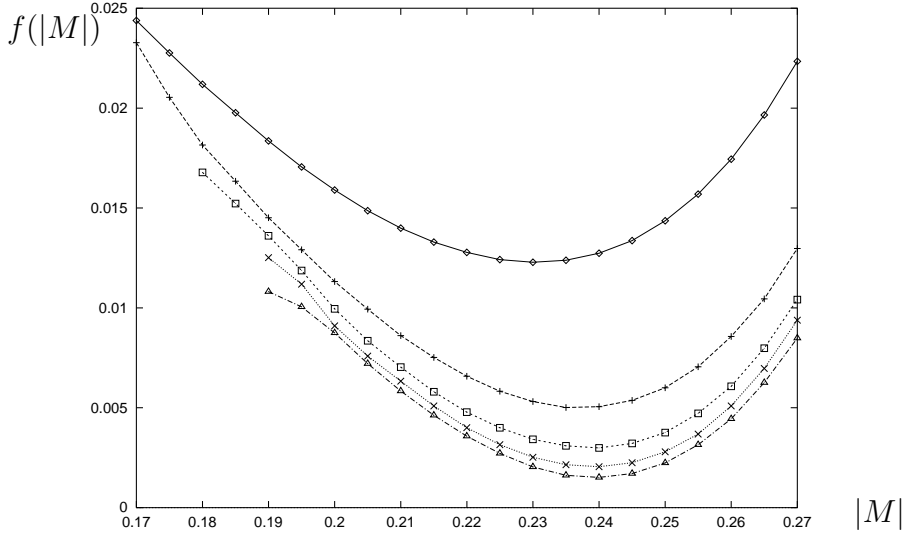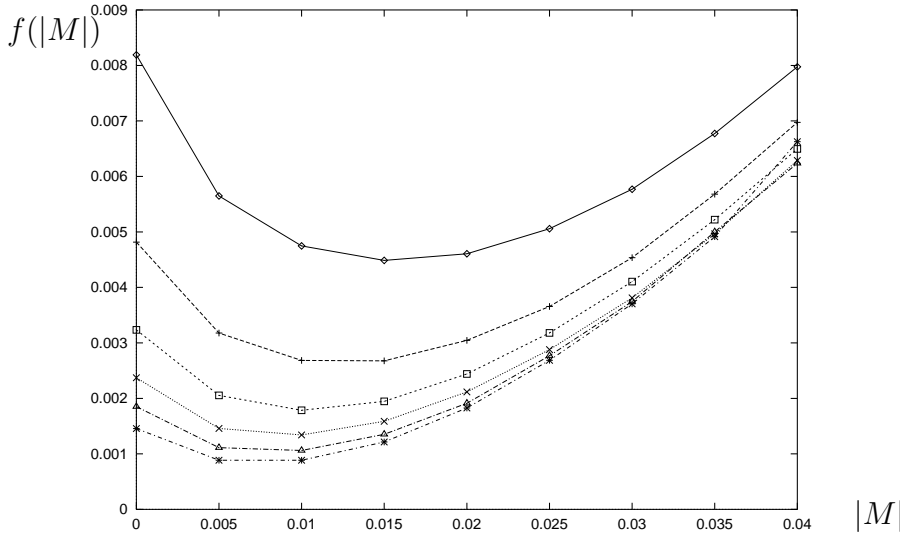

Figure 11. The Ginzburg-Landau potential in the mixed phase ($\rho = 0.2$, $\lambda = 1$, $q = 1.2$) as a function of $|M|$ obtained from Monte-Carlo simulations for $L = 200, 400, 600, 800, 1000$ (from top to bottom).

It is useful to consider the order parameter M defined as follows:

$$M = \frac{1}{L} \sum_{k=1}^{L} \exp(\frac{2\pi i}{L} k) \delta(\beta_k) \tag{7.1}$$

One notices that the order parameter is sensitive only to the vacancies and to the

Figure 12. The Ginzburg-Landau potential in the disordered phase ($\rho = 0.2$, $\lambda = 1$, $q = 2.5$) as a function of $|M|$ obtained from Monte-Carlo simulations for $L = 400, 600, 800, 1000, 1200, 1400$ (from top to bottom).

macroscopic properties of the system (it sees only the lowest frequency). For a given length L of the system we have measured using Monte-Carlo simulations the probability $P(|M|)$ to find a certain value of the modulus of M. Next we have considered the Ginzburg-Landau potential

$$f(|M|) = -\frac{1}{L} \log P(|M|) \tag{7.2}$$

In Ref.[5] we have proven, for another order parameter and another model, that this function converges in the thermodynamical limit. In Figs.10, 11 and 12 this function is shown for the pure, mixed and disordered phases.

These figures confirm know results. Indeed if one has a block of vacancies of length b (again macroscopic length!) a trivial calculation shows that $f(|M|)$ should have a minimum at the value

$$|M|_{\min} = \frac{v}{\pi b} \sin(\pi b) . \tag{7.3}$$

Here v is as usual the density of vacancies. In the pure phase ($b = v$) this gives the value $|M|_{\min} = 0.3027$, for the mixed phase one can use the value $b = 0.675$ obtained using Eq.(6.10) which gives $|M|_{\min} = 0.238$ and, finally, for the disordered phase one gets $|M|_{\min} = 0$ since here $b = 1$ in agreement with the values seen in the figures.

We would like at this point to make, what is in our view, an important observation. In Ref.[5] it was advocated that the Ginzburg-Landau potential defined in Eq.(7.2) is a useful concept not only in equilibrium statistical physics but also in the present context. As one can see from Figs.11 and 12 this is certainly the case for the mixed and disordered
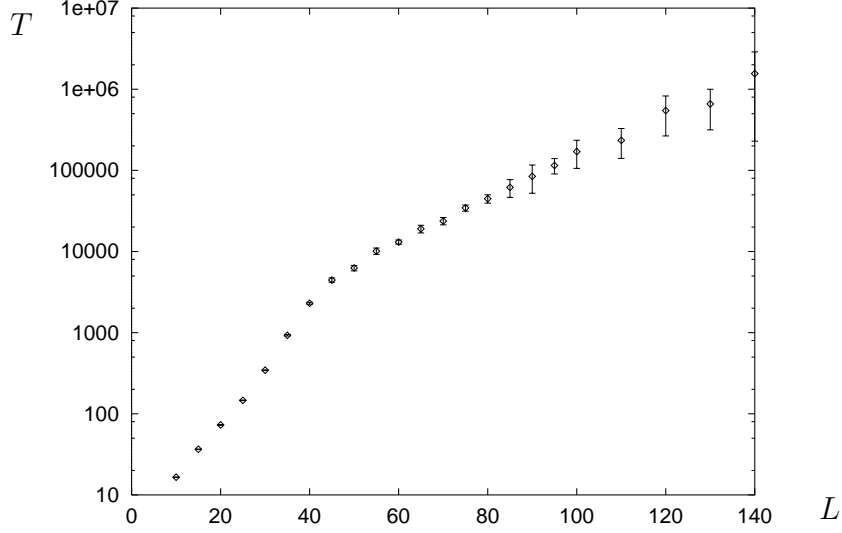
Figure 13. The average flip time T defined in the text as a function of L in the pure phase ($\rho = 0.2$, $\lambda = 1$, $q = 0.8$) obtained from Monte-Carlo simulations.
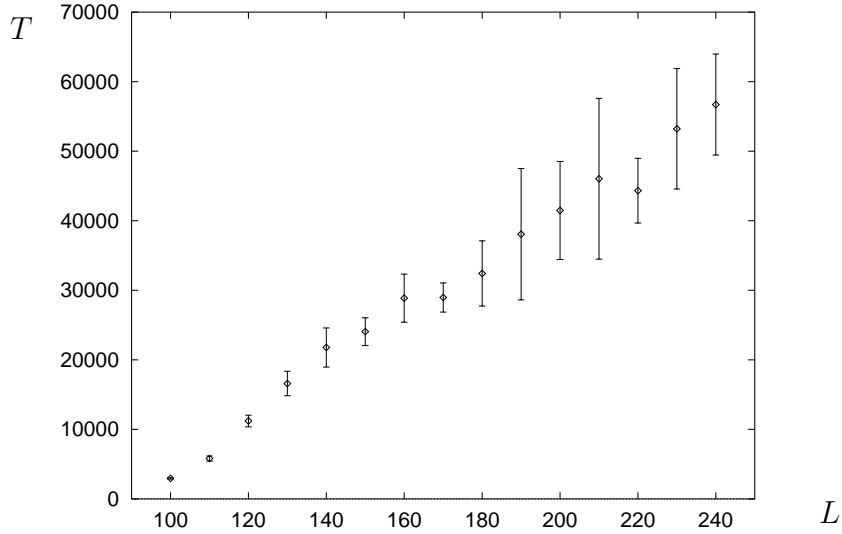

Figure 14. Same as in Fig.13 for the mixed phase ($q = 1.2$).

phases since this function nicely converges for large L. This is not the case for the pure phase. Notice that in this case the function which converges is rather $f(|M|)/L$.

A similar phenomenon occurs for another concept "exported" from equilibrium statistical physics to non-equilibrium, namely the position of the roots of the partition function seen as a function of fugacity [22]. As shown in Ref. [23], they converge to a parabola in the disordered phase, to an ellipse in the mixed phase, but shrink for large L for the pure phase. These observations might be relevant for other models or for the

same model in two dimensions since it might give a way to distinguish between the pure and mixed phases.

In order to obtain new information one can look not to $|M|$ but to M itself and, instead of considering the stationary state only, examine the time dependent behavior of the system. Using Monte-Carlo simulations we have looked for a given size L of the system, at the average flip time T from a configuration which is in the domain $\text{Re}(M) > 0$, $-0.1 < \text{Im}(M) < 0.1$ to a configuration $\text{Re}(M) < 0$, $-0.1 < \text{Im}(M) < 0.1$. Here $\text{Re}(M)$ and $\text{Im}(M)$ represent the real respectively the imaginary parts of M. These average flip times are shown as functions of the size of the system L in Fig.13 (for the pure phase) and in Fig.14 (for the mixed phase). For the pure phase we limited ourselves to $L = 140$ since for larger values of L the flip times are to long. Now we notice a major difference between the two phases: whereas in the pure phase the flip time increases exponentially with L (exponentially increasing barrier), in the mixed phase the flip time increases algebraically. Actually the data are compatible with a linear dependence. This result implies that in the pure phase but not in the mixed phase, translational invariance is spontaneously broken. This settles the problem about the difference between the pure and the mixed phase.

If one uses as a definition of charge segregation the existence of correlation functions which are dependent of the macroscopical variables (y in our notations for the two-point functions), we have to distinguish between the two possibilities put in evidence in this section. One in which one has the breaking of translational invariance, which we propose to call "charge segregation of type B" and one in which translational invariance is not broken which we propose to call "charge segregation of type UB".

We would like to mention that another approach to average flip times in order to put in evidence charge segregation can lead to ambiguous results. A different model was studied in Ref.[24]. The authors looked, (this would correspond to our model), at the average flip time T from a configuration with $b_1|M|_{\min}$ to another with $b_2|M|_{\min}$. Here b_1 and b_2 are L independent constants. They found that T increases exponentially with L. From the shape of the Ginzburg-Landau potential shown in Figs.10 and 11 the same should be true also in our case for both the pure and mixed phases. We could distinguish between the pure and mixed phases only by considering the average flip times in the complex M plane.

We can now continue the analysis of the model and consider the disordered phase.

8.   The disordered phase.

For fixed λ and densities and $q > q_c$ where q_c is given by Eq.(6.29), one finds the disordered phase. In this phase the correlation length is finite. What is the information we have already about this phase?
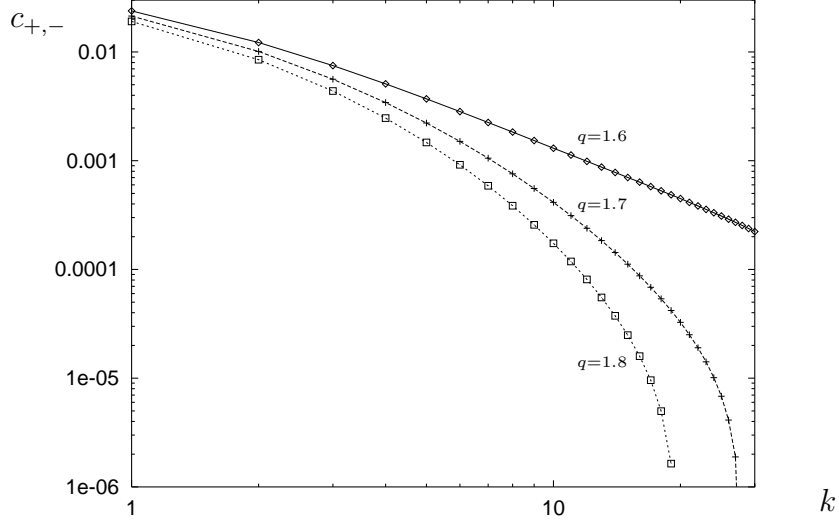
Figure 15. The connected correlation function $c_{+,-}(k)$ as a function of k for for $\rho = 0.2$, $\lambda = 1$, $L = 100$ and three values of q. The data are computed using the grand canonical ensemble.
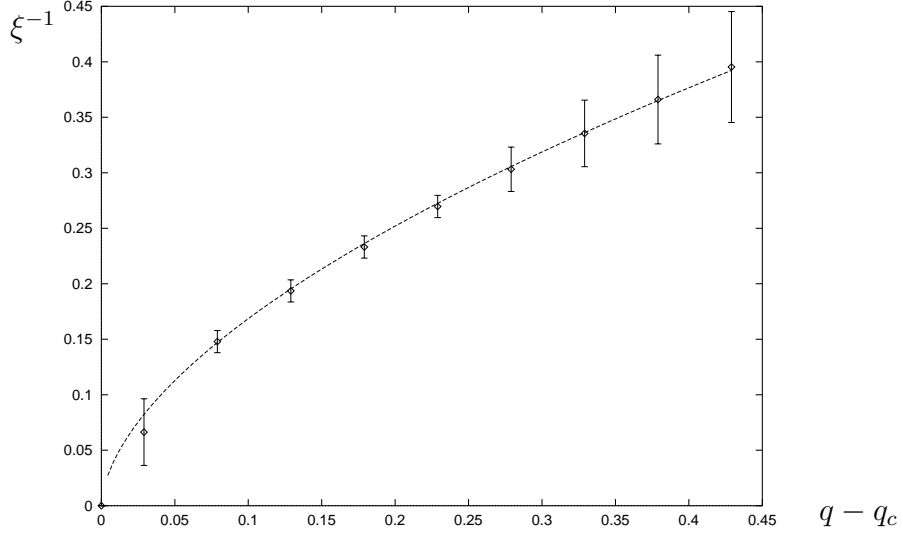

Figure 16. The inverse correlation length as a function of q for $\rho = 0.2$, $\lambda = 1$. The data are obtained determining the correlation lengths from systems of various lengths L (up to 200) and then extrapolating the values to their thermodynamical limit. The dashed curve is given by Eq.(8.3).

a) For large values of q, the current is known (see the large q expansion presented in Sec.2) and is given in the case of equal densities of the charged particles by Eqs.(2.47), (2.53) and (2.56).

b) For λ and q related by the relations (2.12) (those are curves in the q–λ plane
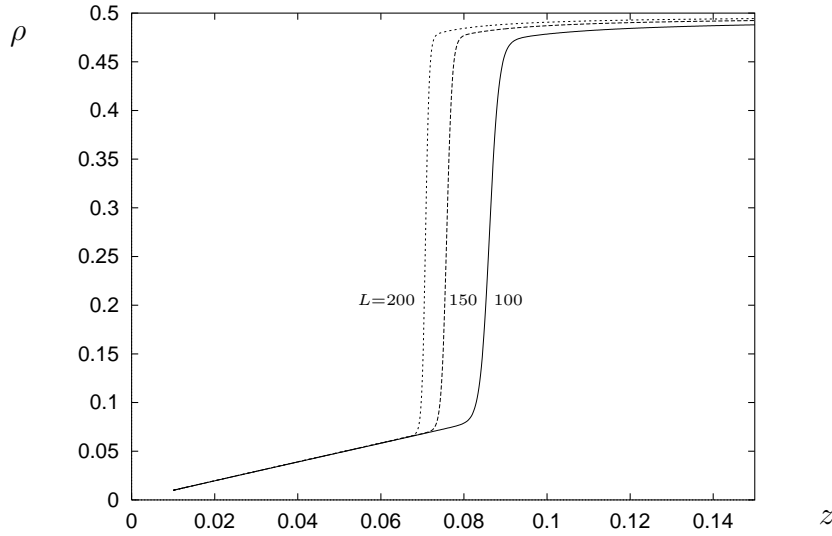
Figure 17. The density ρ as a function of the fugacity z for $q = 1.2$, $\lambda = 1$, $L = 100, 150, 200$ sites.

in the domain where one is in the disordered phase), the quadratic algebra (2.3) has finite-dimensional representations. If the representation is finite-dimensional, it follows that the correlation length is finite. The calculation of various correlation functions is simple but nevertheless tedious. We have not done any calculation of this kind because we didn't expect any surprises.

Since we are interested to understand the nature of the phase transition at q_c, we have taken $\lambda = 1$, $\rho = 0.2$ (for this case we know, using Eq.(6.29), that $q_c = 1.57$) and computed the correlation function $c_{+,-}$ as a function of the microscopic distance k for three values of q. We have taken $L = 100$ and used the grand canonical ensemble. The results are shown in Fig.15 in a double-logarithmic scale. One sees that in the disordered phase ($q = 1.7$ and 1.8) one has an exponential fall-off but that at q_c one has an algebraic one. A fit to the data gives:

$$c_{+,-}(k) = (0.04 \pm 0.01)k^{-1.2 \pm 0.3} \tag{8.1}$$

Next, we were interested in the q dependence of the correlation length. For this purpose, for a given value of q, we have, using the grand canonical ensemble, taken lattices of different lengths L, and determined the correlation length ξ fitting ξ of equation

$$c_{+,-}(k) = A\,k^{-1}\,\exp(-k/\xi) \tag{8.2}$$

The factor k^{-1} was chosen in order to improve the fits to the data. Then we have extrapolated the values of ξ to obtain the large L limit of ξ. These values are shown in Fig.16. As expected the inverse correlation length vanishes at the critical point. As

seen from the figure, the data are compatible with the fit:

$$\xi^{-1} = 0.64 \, (q - q_c)^{0.6} \tag{8.3}$$

At q_c, the correlation length has the following large L behavior:

$$\xi = 0.0065L + 3.98 \tag{8.4}$$

Taking into account that one obtains an excellent fit to the data, the readers who like conformal invariance should give a second thought to this result.

It is obvious that more work is needed in order to fix the values of the two exponents in Eqs.(8.1) and (8.3), check for universality, etc. Our attention however was taken by a problem which we have considered more interesting, namely to understand which symmetry is spontaneously broken at the phase transition. We remind the reader, that the symmetries of the system are translational invariance (for which we have shown in Sec.7 that it is not broken in both the disordered and mixed phase), CP and $U(1) \times U(1)$ corresponding to the conservation of the numbers of positive and negative particles. The answer to this question is given in the next figure.

In Fig.17 we show for $\lambda = 1$ and $q = 1.2$ (which for $\rho = 0.2$ corresponds to the mixed phase but becomes q_c if $\rho = 0.055$), the fugacity(z) dependence on the density(ρ) for three values of L. One notices that the L dependence of the curves suggest that in the thermodynamical limit, ρ increases linearly with z up to the point where ρ reaches the value 0.055 (the linear increase is an empirical observation). At the corresponding value of z, one gets a vertical and z does not fix anymore the density. Such a behavior of the density is known in Bose-Einstein condensation [25] where (there one has a $U(1)$ symmetry) the conservation of the number of particles is broken. In the next section we are going to discuss this topic in detail.

9. Spatial condensation

As is well known, Bose-Einstein condensation is a quantum mechanical phenomenon in which identical particles condensate in a state of zero momentum. This phenomenon takes place in three or more dimensions. In a simple but fascinating one-dimensional stochastic model with a "defect" (reviewed in Appendix C), M. Evans [26] has shown that, choosing the right variables, the probability distribution for the stationary state can be written in terms of occupation numbers with a "dispersion" relation (they are no momenta involved) which give the equivalent of a Bose-Einstein condensation (there is a zero bosonic mode). In this model the condensate corresponds to an empty domain (no particles, just vacancies).

We will pursue the investigation of our model in order to see if indeed more properties are common to the usual Bose-Einstein condensation and to the transition at q_c. The
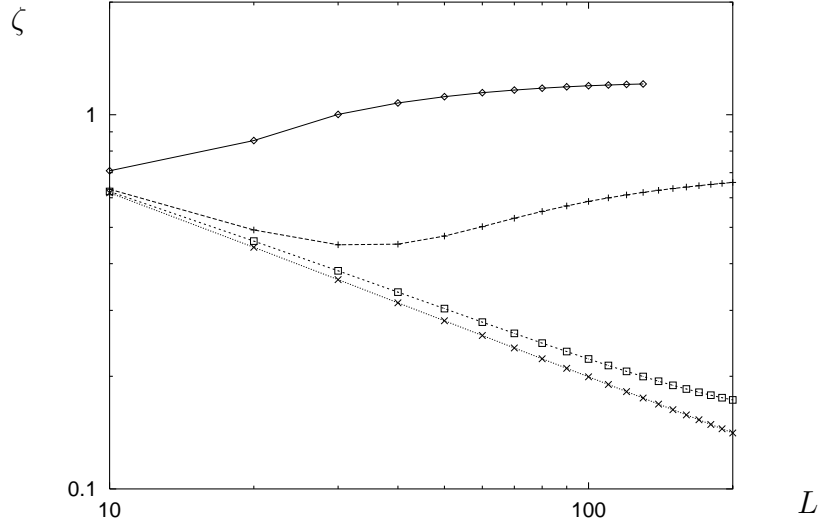
Figure 18. ζ defined by Eq.(9.2) as a function of L for $\rho = 0.2$, $\lambda = 1$ for $q = 0.9$, 1.4, 1.6 and 2.2 (from top to bottom). The data are obtained using the grand canonical ensemble.
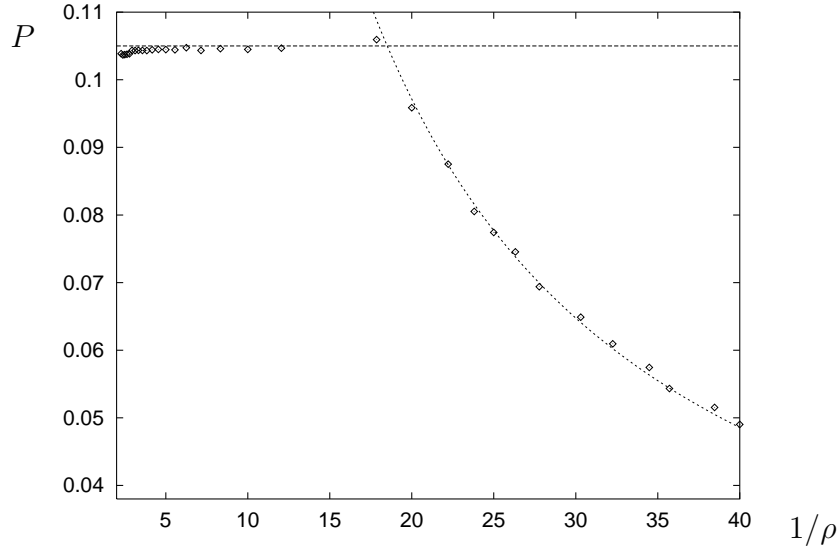

Figure 19. The "pressure" P defined by Eq.(9.3) as a function of $1/\rho$ for $q = 1.2$ and $\lambda = 1$. The data are obtained as explained in the text.

compressibility κ is defined by the relation:

$$\kappa = \zeta^2 L \tag{9.1}$$

where

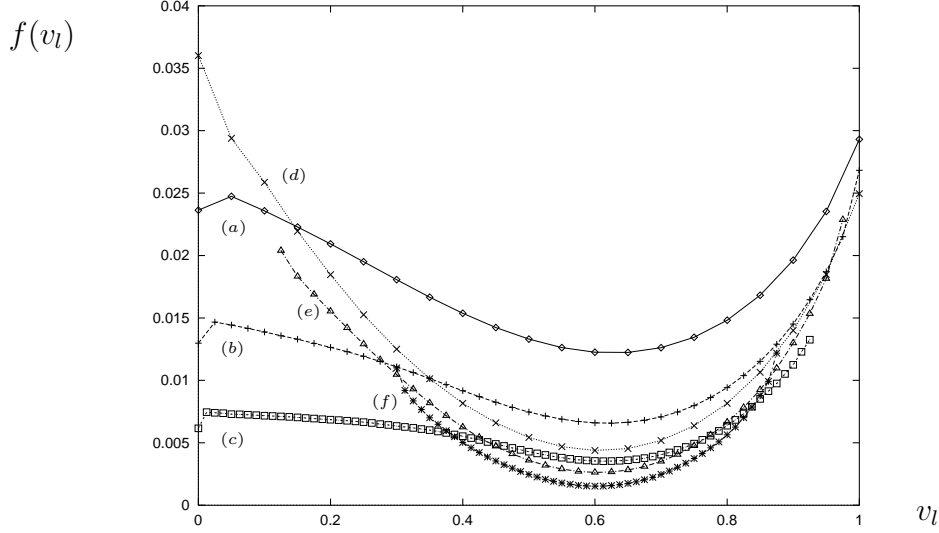$$\zeta = \frac{<(\Delta\rho)^2>^{1/2}}{\rho} \tag{9.2}$$

Figure 20. The Ginzburg-Landau potential $f(v_l)$ as a function of the local density of vacancies v_l. The curves are for $q = 1.6 \approx q_c$ and $L = 400(a), L = 800(b), L = 1600(c)$, and for $q = 2.2$ and $L = 400(d), L = 800(e), L = 1600(f)$. In all cases we have taken $\lambda = 1$ and $\rho = 0.2$.

Using Eq.(2.36) we have measured ζ as a function of L for $\lambda = 1$, $\rho = 0.2$ and several values of q. The data are shown in Fig.18. We notice that for $q = 0.9$ (in the pure phase) and $q = 1.4$ (in the mixed phase), ζ tends to a constant which gives a divergent compressibility. This is not the case in the disordered phase ($q = 2.2$). At the critical point ($q_c = 1.6$) ζ does not decrease like $L^{-1/2}$ but the lattice sizes are too small in order to decide its ultimate behavior.

Another quantity of interest is the "pressure" P, which can be defined as for equilibrium statistical physics:

$$P = \frac{1}{L} \log Z_L^{\mu,\mu} \tag{9.3}$$

and can be determined using Eq.(2.41)

$$J = \lambda z \frac{Z_{L-1}^{\mu,\mu}}{Z_L^{\mu,\mu}} = \lambda z (1 - \frac{\mathrm{d}}{\mathrm{d}L} \log Z_L^{\mu,\mu}) \tag{9.4}$$

Assuming that $\log Z_L^{\mu,\mu}$ is an extensive quantity one obtains:

$$P = 1 - \frac{J}{\lambda z} \tag{9.5}$$

In order to find an "isotherm" (there is no temperature in our problem) we have, for $q = 1.2$ and $\lambda = 1$, computed the current as a function of ρ (at each value of ρ we

have have computed the current for various lattice sizes and extrapolated to large L). The "pressure" was computed using Eq.(9.5) and is shown in Fig.19. There are several interesting things that we can learn from this figure. First that the "pressure" is positive, next that it decreases when the density gets smaller. There are no theoretical reasons that we can think of that can justify why the "pressure" defined by Eq.(9.5) should have the same properties as the pressure in equilibrium systems. Moreover, the "isotherm" shown in Fig.19 looks similar to the isotherm of the free Bose gas when Bose-Einstein condensation takes place.
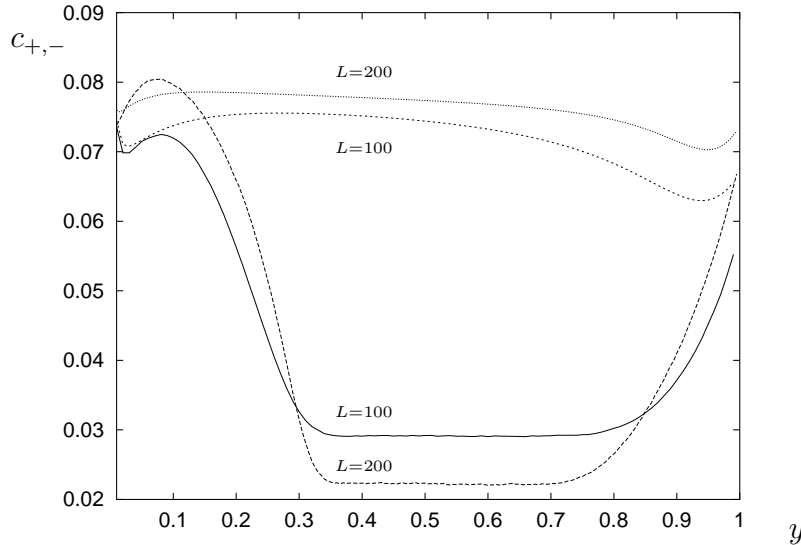

Figure 21. The correlation functions $c_{+,-}$ for the canonical ensemble (bottom, computed by Monte-Carlo simulations) and for the grand canonical ensemble (top) in the mixed phase: $\lambda = 1$, $q = 1.2$, $\rho = 0.2$, $L = 100$ and $L = 200$ sites.

Having in view other systems where spatial condensation might take place we have looked for another method to put it into evidence. We have looked at a given lattice size L at the probability to find a local value of the density of vacancies v_l which is defined as a local average in the macroscopic y coordinate (v_l = number of vacancies in the interval Δy divided by Δy). The corresponding Ginzburg-Landau potential $f(v_l)$ for various values of L with q in the disordered phase and at the critical point is shown in in Fig.20. In the disordered phase ($q = 2.2$) $f(v_l)$ has, as it should, a minimum at $v = 0.6$ which corresponds to the average density. For $q = q_c$ the function $f(v_l)$ is almost flat which would give a Ginzburg-Landau potential corresponding to a first-order phase transition although we know that the transition is second-order. A similar situation occurs also in the case of Bose-Einstein condensation where some thermodynamical quantities behave like in a first-order phase transition [25].

At this point one can ask oneself to which extend the grand canonical ensemble is useful at all in the mixed phase (we have used it consistently to compute the current).
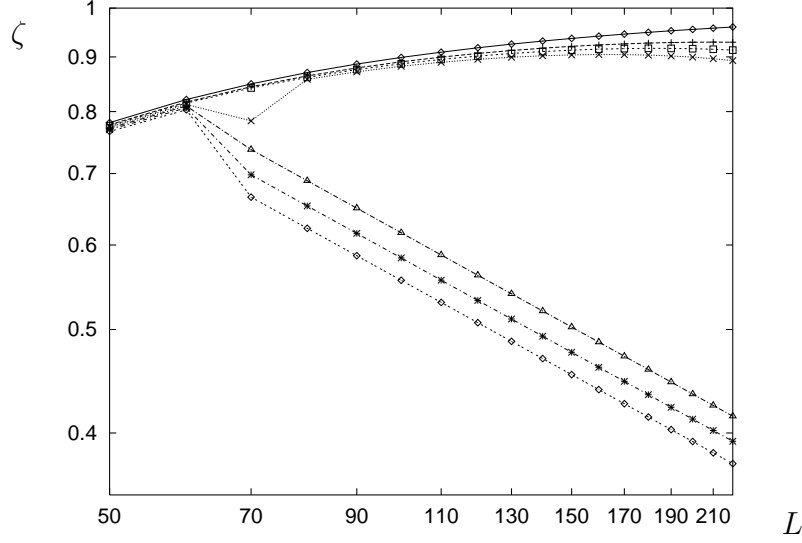
Figure 22. ζ defined by Eq.(9.2) as a function of L for $\rho = 0.2$, $\lambda = 1$ and $q = 1.2$ for various values of ν (from top to bottom $\nu = 0, 0.05, 0.06, 0.07, 0.08, 0.09, 0.1$)
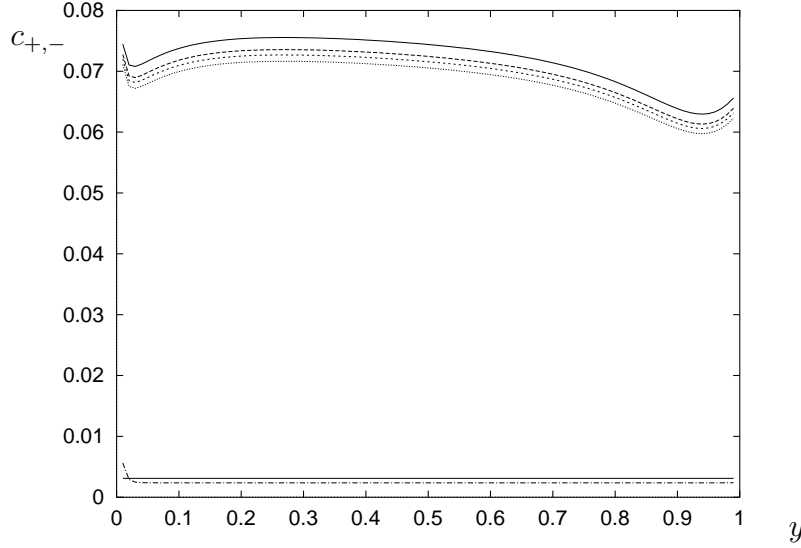

Figure 23. The correlation function $c_{+,-}$ as a function of y for $\rho = 0.2$, $\lambda = 1$ $q = 1.2$, $L = 100$ and various values of $\nu = 0, 0.05, 0.06, 0.07, 0.08$ (from top to bottom). The solid line corresponds to the fluid (see the text).

It turns out that if one wants to compute local quantities like the current or other local two-point functions (see Fig.3), the grand canonical ensemble gives correct results. We have to keep in mind that the finite-size effects are of order L^{-1} (see Eq.(3.9)) as opposed to L^{-2} for the canonical ensemble (see Eq.(6.26)). If, however, one is interested in the values of the correlation functions at fixed macroscopic distances y (see the definition in Eq.(4.3)) using the grand canonical ensemble one gets wrong results. In order to

illustrate this point, in Fig.21 we compare the values of the correlation function $c_{+,-}$ obtained using the grand canonical ensemble and the canonical ensemble (Monte-Carlo simulations) in the mixed phase. We notice that around $y = 0$ or 1, the two methods give the same results but that the results differ drastically otherwise.

Can the grand canonical still be used in order to get information about the mixed phase? We believe that the answer is yes and we have explored this possibility. The idea is inspired by the way the problem is solved for the usual Bose-Einstein condensation (the procedure is shortly repeated in Appendix C). There, one introduces in the Hamiltonian a supplementary term, which breaks the $U(1)$ symmetry of the problem, proportional with a constant ν and the square of the volume. After a Bogoliubov transformation, the net effect is a modification of the partition function given by the grand canonical ensemble by a factor which depends on the volume, ν and the chemical potential. This changes the relation between the density and the chemical potential. In order to compute a physical quantity, one keeps ν fixed, then one takes the volume to infinity and at the end, makes ν equal to zero. Since in our case we were not able to find a way to break explicitly the $U(1) \times U(1)$ symmetry of the problem, we have, in analogy with what is done for the Bose-Einstein gas, just modified the the partition function (2.32) of the grand canonical ensemble by a factor which takes into account that we have two chemical potentials and that at the critical point the chemical potential is not zero:

$$Z_L^{\mu_1,\mu_2}(\nu) = \exp(\frac{L\nu^2}{2\mu_c - \mu_1 - \mu_2})Z_L^{\mu_1,\mu_2} \tag{9.6}$$

In Fig.22 we show the L dependence of ζ defined by Eq.(9.2) in the mixed phase for various values of ν. We have to keep in mind that the range of values of L is limited. For $\nu = 0$, 0.05, 0.06 and 0.07 it looks like the compressibility κ (see Eq.(9.1) diverges. A dramatic change takes place for $\nu = 0.08$, the compressibility becomes convergent. It is plausible to assume that the compressibility converges for any non-vanishing ν (one has to take larger lattices to observe the phenomenon). We further investigate the effect of the modification of the partition function. In Fig.23 we show again the the correlation function $c_{+,-}$ as a function of y (compare with Fig.21), but this time for various values of ν.

We notice that between $\nu = 0.07$ and $\nu = 0.08$ again a dramatic change takes place: the correlation function (it is not the connected one!) drops to a constant value. It is tempting to assume that this should be the correlation in the fluid observed in the mixed phase (the symmetry breaking term eliminates the condensate also in the case of the Bose-Einstein gas). This would imply:

$$c_{+,-} = R_+^{\text{fl}} R_-^{\text{fl}} = (R_+^{\text{fl}})^2 \tag{9.7}$$

where R_+^{fl} is given by Eq.(6.38). Using Eq.(6.10) this gives $c_{+,-} = 0.031$. This is the solid line shown in Fig.23 which gives approximately the correlation function observed

for $\nu = 0.08$.

It is obvious that this investigation is only preliminary but we believe that it gives the right approach to derive the properties of the fluid in the mixed phase. It also shows how similar are the condensation phenomenon in the Bose-Einstein gas and in our model.

10.   Conclusions

We believe that we brought some more light in the understanding of phase transitions in one-dimensional stationary states. The model we considered has two advantages: it has interesting physical properties and has behind it a mathematical structure given by a quadratic algebra. This mathematical structure is not only a useful computational tool but allows, due to its similarity to the mathematical formulation of equilibrium statistical physics, to define relevant quantities which characterise the nature of the phase transition. A first example is the definition of the grand canonical ensemble. Working with this ensemble has not only allowed to obtain exact results (like the large q expansion presented in Sec.2.4) but also to do precise numerical calculations on large lattices. Moreover, it allowed to define the analogue of the pressure which, amazingly, has the same properties as in equilibrium (see Fig.19). Using the grand canonical ensemble we were able to identify the nature of the phase transition between the disordered and the mixed phase since this transition resembles the one seen in the Bose-Einstein condensation (see the fugacity dependence of the density in Fig.17 and the volume dependence of the compressibility in Fig.18). Most importantly, using the grand canonical ensemble, one can break explicitly the continuous symmetries of the problem (conservation of the number of charged particles) in analogy with the treatment of the same problem in the case of Bose-Einstein condensation (see Eq.(9.6) and Figs.22 and 23).

Before discussing the physics of the model, we would like to stress some other results presented in this paper. We have shown that the Ginzburg-Landau potential, introduced earlier in Ref.[5] to study first-order phase transitions, is a meaningful quantity also in the present context. This was checked for two order parameters (see Figs.11, 12 and 20) and the behavior of this function in the case of a second-order phase transition was for the first time observed. The Ginzburg-Landau potential can also be useful in order to put in evidence the breaking of translational invariance since in this case it does not converge in the infinite volume limit. This observation is based only on the data presented in Fig.10 and obviously one needs to do more work to clarify this point.

We think that we have also found the proper method to look at flip times in order to distinguish between situations when one has charge segregation with and without translational symmetry breaking. As described in Sec.7, one has to look not only at the

module of the order parameter defined by Eq.(7.1) but also at its phase.

Inspired by the numerical results presented in Appendix B, in Sec.6 we have shown in detail how to do mean-field calculations for this model. The present method can also be used for a larger class of models. These mean-field equations are two coupled non-linear differential equations (see Appendix B). The fact that one is able to find analytic solutions for the stationary states is very non-trivial. We will return to this topic in Ref.[7] where we consider the case of different densities of positive and negative particles. We will explain why the differential equations should be called the two-component Burgers equations and give more analytic solutions of these equations.

We found the physics of this simple model fascinating. There are two phase transitions. One separates the disordered and mixed phases and is of second-order. This phase transition is related to spatial condensation. We got estimates for several critical exponents related to the inverse correlation length, the algebraic behavior of the two-point function at the phase transition and finite-size scaling corrections (see Secs.6 and 8). The mixed phase with its simple expression for the current and its independence on the density and other parameters as well as the bumps well described by mean-field are nice pieces of physics. The nature of the bump is also interesting: one has two open systems glued together. One, the condensate composed of charged particles is well understood from the corresponding two-state problem. About the second, the fluid, we know little except for the fact that it shows no macroscopic structure. Actually, one major difference between Bose-Einstein condensation and spatial condensation is that here the condensate has a simple structure whereas the fluid phase is interesting since it is different than the disordered phase and hence worth studying.

In another publication [27] where we consider the open system with the same bulk rates as in the present one we will show that a first-order phase transition occurs between one phase which is the condensate and a second one which is the fluid. In this way one can get directly more information about both phases.

Unfortunately we did not pay much attention to the second phase transition, the one between the mixed and pure phase, where translational invariance is spontaneously broken.

This work has left us with quite a few open questions which we would like to address in some future publications:

(a) We have not touched the study of the model in the case of different densities. A second paper will be devoted to this.

(b) The algebraic approach and the Monte-Carlo simulations were used only for a limited numbers of points in the q–λ plane. Most of our conclusions including the transition separating the mixed phase form the disordered phase are mean-field results which were therefore checked only in a limited region of the q–λ plane. This does not mean that in other regions mean-field is valid.

(c) The dynamics of the model with the parameters chosen such that the stationary states correspond to the pure and mixed phases as well as at the phase transition points can lead to plenty of interesting results.

(d) Last but not least, there is many information given in this paper which deserve a more accurate research. We did our best but we feel that this is not enough.

Acknowledgments

Appendix A.   The connection between the representations of the quadratic algebra and of the quantum algebra $U_q so(2,1)$. Recurrence relations.

The expressions (2.7)-(2.10) of the representations of the quadratic algebra (2.3) suggest to any reader familiar with the representations of quantum algebras a connection between these very different mathematical topics. This connection is for the purposes of this paper not only a mathematical curiosity but, as will be seen, one can write recurrence relations for physical relevant quantities which have an interpretation from the quantum algebras point of view. We will comment about these recurrence relations at the end of this Appendix.

We first remind the reader of the definition of the quantum algebra $U_s o(2,1)$. This is the deformation given by a parameter s of the well known algebra $so(2,1)$. (The deformation parameter is usually denoted by q but this symbol is already used in this paper). The quantum algebra is defined by three generators k, e and f satisfying the relations [28]:

$$
\begin{aligned}
[e,f] &= \frac{k^2 - k^{-2}}{s - s^{-1}} \\
k\,e\,k^{-1} &= s^{-1}e \\
k\,f\,k^{-1} &= s\,f
\end{aligned}
\tag{A.1}
$$

One representation of this algebra has the following matrix elements:

$$k = \begin{pmatrix} k_1 & 0 & 0 & 0 & \cdots \\ 0 & k_2 & 0 & 0 & \\ 0 & 0 & k_3 & 0 & \\ 0 & 0 & 0 & k_4 & \\ \vdots & & & & \ddots \end{pmatrix} \qquad e = \begin{pmatrix} 0 & u_1 & 0 & 0 & \cdots \\ 0 & 0 & u_2 & 0 & \\ 0 & 0 & 0 & u_3 & \\ 0 & 0 & 0 & 0 & \ddots \\ \vdots & & & & \ddots \end{pmatrix}$$

$$f = \begin{pmatrix} 0 & 0 & 0 & 0 & \cdots \\ v_1 & 0 & 0 & 0 & \\ 0 & v_2 & 0 & 0 & \\ 0 & 0 & v_3 & 0 & \\ \vdots & & \ddots & \ddots & \end{pmatrix} \tag{A.2}$$

where

$$k_j = s^j, \qquad u_j \, v_j = [j]_s \, [j+1]_s \tag{A.3}$$

and

$$[j]_s = \frac{s^j - s^{-j}}{s - s^{-1}} \, . \tag{A.4}$$

Notice that if

$$s^2 = r = \frac{1}{\lambda} \tag{A.5}$$

then G_1 and G_2 (see Eq.(2.7)) can be expressed in terms of k, e and f as follows:

$$G_1 = \frac{k}{s}\left(e + \frac{k - k^{-1}}{s - s^{-1}}\right), \qquad G_2 = \frac{k}{s}\left(f + \frac{k - k^{-1}}{s - s^{-1}}\right) \tag{A.6}$$

In order to show how the connection between the representation of the quadratic algebra and the quantum group can be used, we will consider a simpler example where $s = 1$ (this is the familiar case of the $so(2,1)$ algebra). In this case, one has:

$$G_1 = S^z + S^-, \qquad G_2 = S^z + S^+ \tag{A.7}$$

with:

$$\begin{aligned} S^z \, |k> &= k \, |k> \\ S^- \, |k> &= \sqrt{k(k-1)} \, |k-1> \\ S^+ \, |k> &= \sqrt{k(k+1)} \, |k+1> \end{aligned} \tag{A.8}$$

where $k \geq 1$. We have to keep in mind (see Eq.(2.8)) that the matrix G_0 has a simple expression:

$$G_0 \, |k> = \delta_{k,1} \, |k> \tag{A.9}$$

The calculation of the current for example, in the grand canonical ensemble, implies the calculation of the quantity (see Eqs. (2.32)-(2.34)):

$$C^N |1> \tag{A.10}$$

where

$$C = G_0 + (z_1 + z_2)S^z + z_1 S^- + z_2 S^+ \tag{A.11}$$

Writing $C^N |1>$ in the $|n>$ basis:

$$C^N |1> = \sum_{n=1}^{N} t_n^{(N)} |n> \tag{A.12}$$

one can find a recurrence relation for the $t_n^{(N)}$ using (A.8) and (A.9). It is useful to denote:

$$\sqrt{n}\, t_n^{(N)} = u_n^{(N)} \tag{A.13}$$

and we get the following recurrence relations for $2 \le n \le N - 1$:

$$
\begin{aligned}
u_1^{(N+1)} &= (1 + z_1 + z_2)\, u_1^{(N)} + z_1\, u_2^{(N)} \\
\frac{1}{n}\, u_n^{(N+1)} &= (z_1 + z_2)\, u_n^{(N)} + z_1\, u_{n+1}^{(N)} + z_2\, u_{n-1}^{(N)} \\
\frac{1}{N}\, u_N^{(N+1)} &= (z_1 + z_2)\, u_N^{(N)} + z_2\, u_{N-1}^{(N)} \\
\frac{1}{N+1}\, u_{N+1}^{(N+1)} &= z_2\, u_N^{(N)}
\end{aligned}
\tag{A.14}
$$

If in the recurrence relations (A.14) one drops the 1 in the term $(1 + z_1 + z_2)$ one obtains recurrence relations defined only by the algebra $so(2,1)$. Similar recurrence relations can be found also in the deformed case (s different from 1). We just did not have the time to exploit the recurrence relations just mentioned, they might appear however in a further publication.

Before closing this Appendix let us observe that for

$$q = \frac{1}{r} = \lambda + 1 \tag{A.15}$$

G_1 and G_2 can be expressed through the generators of the r deformed bosonic creation and annihilation operators:

$$G_1 = 1 + \sqrt{1 - r}\, a, \qquad G_2 = 1 + \sqrt{1 - r}\, a^+ \tag{A.16}$$

where

$$a\, a^+ - r\, a^+ a = 1 \tag{A.17}$$

and

$$a\, |1> = <1|\, a^+ = 0 \tag{A.18}$$

This allows again to write recurrence relations like (A.14) with a clear mathematical meaning.

In defining the grand canonical ensemble (see Sec. 2) we had to make a choice between isomorphic algebras (Eqs.(2.33)–(2.34)) corresponding to different normalizations of the generators G_0, G_1 and G_2. As we can see from Eqs.(A.8) and (A.16), the chosen normalisation corresponding to Eq.(2.30) looks reasonable.

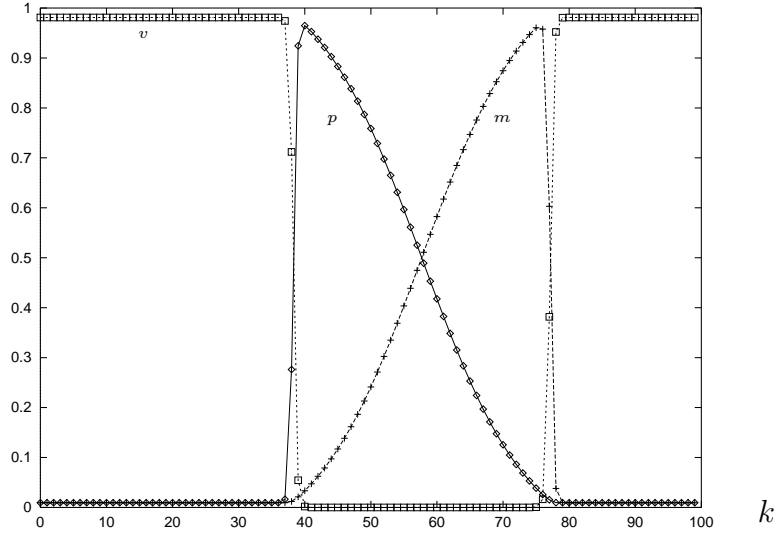## Appendix B.   Mean-field on the lattice and in the continuum

Figure B1.   The inhomogeneous solution of the mean-field equations in the pure phase for $q = 0.9$, $\lambda = 1$, $p = m = 0.2$ and $L = 100$.

Let p_k, m_k and v_k be the average concentrations on the site k of positive. negative particles and vacancies. Neglecting correlations, the expression of the currents of positive and negative particles on the link between the sites k and $k+1$ are:

$$
\begin{aligned}
J^+_{k,k+1} &= q\,p_k m_{k+1} - m_k p_{k+1} + \lambda\,p_k(1 - m_{k+1} - p_{k+1}) \\
J^-_{k+1,k} &= q\,p_k m_{k+1} - m_k p_{k+1} + \lambda\,m_{k+1}(1 - m_k - p_k)
\end{aligned}
\tag{B.1}
$$

The time evolution of the local densities can be derived from the master equation:

$$
\begin{aligned}
\frac{\mathrm{d}}{\mathrm{d}t}p_k &= J^+_{k-1,k} - J^+_{k,k+1} \\
\frac{\mathrm{d}}{\mathrm{d}t}m_k &= J^-_{k+1,k} - J^-_{k,k-1}
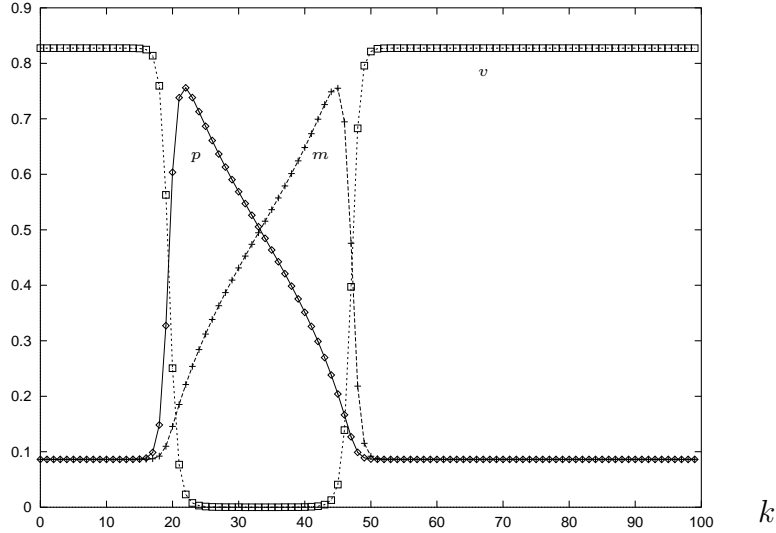\end{aligned}
\tag{B.2}
$$

Figure B2. Same as in Fig.B1 for the mixed phase for $q = 1.2$, $\lambda = 1$, $p = m = 0.2$ and $L = 100$.

For the stationary state one gets a system of nonlinear equations for the local concentrations which might give several solutions. In order to find them, we have proceeded as follows. We have used Eq.(B.2) taking discrete values for the time and chose the parameters (q, λ and ρ) corresponding to the pure and mixed phase. As an initial distribution we have put at random ρL positive and ρL negative particles on the lattice. Starting from one of these configuration the iteration converges either to the homogeneous solution ($p_k = m_k = \rho$) or to inhomogeneous solutions. The inhomogeneous solutions have all the same profiles which differ only in their position on the ring. Therefore, in mean-field, translational invariance is broken in both the pure and mixed phases even for finite L. In Figs. B1 and B2 the inhomogeneous solutions are shown for the pure and mixed phase. In both figures one sees two domains. In one domain one has only charged particles with non-uniform distributions (the condensate) and in the other domain one has uniformly distributed vacancies and charged particles (the fluid). For a given values of the parameters q, λ and ρ, the inhomogeneous solution appears only for a lattice size $L > L_{\min}$. For larger lattice sizes, one finds inhomogeneous solutions different of those shown if Figs.B1 and B2. Namely if $L > 2L_{\min}$ one finds solutions looking like two pictures shown in Fig.B2 glued together (the same is true for the pure phase). Otherwise speaking, for a lattice size $2L$ one gets a solution with two condensates, in each condensate one sees the same concentrations profiles as in the case of a single condensate for a lattice size L. The reader can guess what happens for

$L > 3L_{\min}$. Based on this observations, we now look at the mean-field equations in the continuum.

Instead of the Eqs.(B.1) for the currents, one gets:

$$J^+ = (q-1)\rho_+\rho_- + \lambda\rho_+\rho_0$$
$$+ \frac{1}{2L}\left((q+1)(\rho_+\frac{\partial\rho_-}{\partial y} - \rho_-\frac{\partial\rho_+}{\partial y}) + \lambda(\rho_+\frac{\partial\rho_0}{\partial y} - \rho_0\frac{\partial\rho_+}{\partial y})\right)$$
$$J^- = (q-1)\rho_+\rho_- + \lambda\rho_-\rho_0$$
$$+ \frac{1}{2L}\left((q+1)(\rho_+\frac{\partial\rho_-}{\partial y} - \rho_-\frac{\partial\rho_+}{\partial y}) + \lambda(\rho_0\frac{\partial\rho_-}{\partial y} - \rho_-\frac{\partial\rho_0}{\partial y})\right) \qquad \text{(B.3)}$$

where ρ_+, ρ_- and ρ_0 are the densities of positive, negative particles and vacancies,

$$\rho_+(y) + \rho_-(y) + \rho_0(y) = 1 \qquad \text{(B.4)}$$

The Eqs.(B.2) are replaced by:

$$\frac{\partial\rho_+}{\partial t} = -\frac{\partial J^+}{\partial y}, \qquad \frac{\partial\rho_-}{\partial t} = \frac{\partial J^-}{\partial y} \qquad \text{(B.5)}$$

The solutions of the Eqs.(B.5) have to be positive, fulfill Eq.(B.4) as well as

$$\int_0^1 \rho_+(y)\,\mathrm{d}y = p, \qquad \int_0^1 \rho_-(y)\,\mathrm{d}y = m \qquad \text{(B.6)}$$

Notice that solutions of the mean-field equations will depend on the parameters L, q, λ, p and m.

A more detailed study of the solutions of Eq.(B.5) will be presented elsewhere [7], in the present paper we are interested in the stationary solutions which are obtained when $p = m$ and with only one condensate. These solutions are obtained in Sec.6 based on the observation that in the condensate one has only two species which makes the problem solvable and that in the fluid the concentrations are uniform. It turns out that in the presence of fluctuations only the solutions with one condensate are relevant for the stationary states.

Appendix C.   Bose-Einstein condensation in equilibrium and spatial condensation in stationary states.

We will first review the phenomenon of condensation for the free Bose gas [29]. The partition function Z of the system is:

$$Z = \mathrm{Tr}\,\exp-\beta\sum_{\vec{k}}\left((\epsilon(\vec{k}) - \mu)n_{\vec{k}} - \sqrt{V}\nu(a_0 + a_0^+)\right) \qquad \text{(C.1)}$$

where β is the inverse of the temperature, $\epsilon(\vec{k})$ is the energy, $\vec{k}$ the momentum, μ the chemical potential, V the volume, ν gives the intensity of the symmetry breaking term

and $n_{\vec{k}}$ is the occupation number:

$$n_{\vec{k}} = a_{\vec{k}}^+ a_{\vec{k}} \tag{C.2}$$

The $a_{\vec{k}}$'s are Bosonic annihilation operators. We assume for simplicity that we consider the three-dimensional gas with a quadratic dispersion relation so that one has Bose-Einstein condensation. Since $\epsilon(0) = 0$ we have a zero Bosonic mode. In the absence of the symmetry breaking term ($\nu = 0$), the Hamiltonian is invariant under $U(1)$ transformations

$$a_0 \rightarrow a_0 \, e^{i\phi} \tag{C.3}$$

where ϕ is a phase. Through the non-unitary Bogoliubov transformation

$$b_0 = a_0 + \sqrt{V}\frac{\nu}{\mu} \tag{C.4}$$

the partition function becomes

$$Z = e^{-\frac{\beta V \nu^2}{\mu}} \mathrm{Tr} \, \exp - \beta \sum_{\vec{k}} \left(\epsilon(\vec{k}) - \mu) \tilde{n}_{\vec{k}} \right) \tag{C.5}$$

where $\tilde{n}_{\vec{k}}$ are again number operators ($\tilde{n}_{\vec{k}} = 0, 1, 2, \ldots$)

$$\tilde{n}_{\vec{k}} = b_{\vec{k}}^+ b_{\vec{k}} \tag{C.6}$$

The net effect of the Bogoliubov transformation is the appearance of the chemical potential not only under the trace operation but also in the overall factor. This implies that ρ defined by the expression

$$\rho = \frac{1}{V\beta} \frac{\partial}{\partial \mu} \log Z \tag{C.7}$$

is the average density of particles only for $\nu = 0$. The main point is that we first do the calculation for ν different from zero, take the infinite volume limit and only at the end let ν vanish. In this way one gets the thermodynamical properties of the gas also under the critical temperature since the condensate (which is a state of zero momentum) disappears from the calculation as a consequence of the symmetry breaking term. This method can also be seen as a regularization procedure.

That the free Bose gas is a quantum system (the expression (C.5) contains only occupation numbers which are c-numbers) can be seen once we compute measurable correlation functions like

$$g(\vec{r}_1, \vec{r}_2) = <\psi(\vec{r}_1)\psi^\dagger(\vec{r}_2)> \tag{C.8}$$

where

$$\psi(\vec{r}) = \frac{1}{\sqrt{V}} \sum_{\vec{k}} e^{i\vec{k}\vec{r}} a_{\vec{k}} \tag{C.9}$$

since the creation and annihilation operators verify the Heisenberg algebra. That much on the Bose-Einstein gas.

In the case of the spatial condensation which appears in the mixed phase, the condensate is separated in space from the fluid and not in momentum space. The simplest model of spatial condensation that we know of is the model with a "defect" of Ref. [26]. In this model M particles hop in a totally asymmetric way with a rate 1 on a ring with L sites and one particle (the "defect") hops with a rate p (with $p < 1$). It was shown that the partition function for the grand canonical ensemble is

$$Z = \sum_{n_0, n_1, \dots} \delta(\sum_{k=0} n_k - L) \frac{1}{p^{n_0}} \exp\left(\mu \sum_{k=0} n_k\right) \tag{C.10}$$

where $n_0, n_1, n_2, \dots$ are the number of vacancies in front of the defect, of particle 1, particle 2 etc. Obviously,

$$L - (M + 1) = \frac{\partial}{\partial \mu} \log Z \tag{C.11}$$

At low density of particles (large density of vacancies), the particles produce a jam behind the defect and the string of vacancies (of length n_0) in front of the defect can be seen as a condensate. The expression (C.10) looks similar to (C.1) with at least two major differences: the occupations numbers n_k are constrained by the length L of the chain (we have condensation in real space and not in momentum space!) and there are no measurable correlation functions given by creation and annihilation operators in this problem.

In the model discussed in present paper, the analogy between the expression of the partition functions (2.32) for the stationary state and (C.1) for the Bose gas is completely obscure. Some similarities do exist. The algebra (2.2) plays a role similar to the Heisenberg algebras hidden in the occupation numbers appearing in the Bose gas and the transformation (2.4) representing the conservation of the numbers of positive and negative particles (we have a $U(1) \times U(1)$ symmetry in our case) corresponds to the transformation (C.3). We were not able to bring more understanding in the symmetry breaking mechanism using the algebraic approach although we wish we had, since we were looking for an equivalent of the Bogoliubov transformation in oder to eliminate the condensate. Our approach using Eq.(9.6) can be seen at this stage as an educated guess to do the regularisation.

References

[1] B. Derrida, E. Domay and D. Mukamel 1992, *J.Stat.Phys.* **69** 667

[2] G. Schütz and E. Domany 1993, *J.Stat.Phys.* **72** 277

[3] B. Derrida, M.R. Evans, V. Hakim and V. Pasquier 1993, *J. Phys. A: Math. Gen.* **26** 1493

58

[4] M.R. Evans, D.P. Foster, C. Godrèche and D. Mukamel 1995, *Phys. Rev. Lett.* **74** 208; *J.Stat.Phys.* **80** 69

[5] P.F. Arndt, T. Heinzel and V. Rittenberg 1998, *J.Stat.Phys.* **90** 783

[6] P.F. Arndt, T. Heinzel and V. Rittenberg 1998, *J. Phys. A: Math. Gen.* **31** L45

[7] P.F. Arndt and V. Rittenberg, *Spontaneous Breaking of Translational Invariance and Spatial Condensation in Stationary States on a Ring. II. The Charged System and the Two-component Burgers Equation.*, to be published

[8] F.H.L. Eßler and V. Rittenberg 1996, *J. Phys. A: Math. Gen.* **29** 3375

[9] M.R. Evans, Y. Kafri, H.M. Koduvely and D. Mukamel 1998, *Phys. Rev. Lett.* **80** 425; *Phys. Rev.* E**58** 2764

[10] G. Korniss and B. Schmittman 1997, *Phys.Rev.* **E56** 4072

[11] P.F. Arndt, T. Heinzel and V. Rittenberg 1998, *J. Phys. A: Math. Gen.* **31** 833

[12] I. Affleck, T. Kennedy, E.H. Lieb and H. Tasaki 1987, *Phys. Rev. Lett.* **59** 799

[13] V. Hakim and J.P. Nadal 1983, *J. Phys. A: Math. Gen.* **16** L213

[14] M. Henkel and G. Schütz 1988, *J. Phys. A: Math. Gen.* **21** 2617

[15] B. Derrida, S.A. Janowsky, J.L. Lebowitz, and E.R. Speer 1993, *J. Stat. Phys.* **73** 813

[16] R. Schmittman, K. Hwang and R.K.P. Zia 1992, *Europhys.Lett.* **19** 19

[17] D.P. Foster and C. Godrèche 1994, *J.Stat.Phys.* **76** 1129

[18] J. Krug 1991, *Phys. Rev. Lett.* **67** 1882

[19] M. Barber 1973, "Finite-Size Scaling", in *Phase Transitions and Critical Phenomena Vol.8*, Eds. C. Domb and J.L. Lebowitz (Academic Press)

[20] F.C. Alcaraz, S. Dasmahapatra and V. Rittenberg 1998, *J. Phys. A: Math. Gen.* **31** 845

[21] S. Ramaswamy and M. Barma 1987, *J. Phys. A: Math. Gen.* **20** 2973

[22] C.N. Yang and T.D. Lee 1952 *Phys. Rev.* **87** 404, 410

[23] P.F. Arndt, to be published

[24] R. Lahri and S. Ramaswamy 1997, *Phys. Rev. Lett.* **79** 1150

[25] R.K. Pathria 1972 *Statistical Physics* (Pergamon, Oxford)

[26] M.R. Evans 1996, *Europhys.Lett.* **36** 13

[27] P.F. Arndt and V. Rittenberg, *The AHR model with open boundaries*, to be published

[28] T. Masuda, K. Mimachi, Y. Nakagami, M. Noumi, Y. Saburi and K. Ueno 1990, *Lett.Math.Phys.* **19** 195

[29] J.D. Gunton and M.J. Buckingham 1968, *Phys.Rev.* **166** 152